Journal of Innovative Optical Health Sciences
Vol. 11, No. 6 (2018) 1830003 (20 pages)

DOI: 10.1142/S1793545818300033

World Scientific
www.worldscientific.com



# Black phosphorus: A novel nanoplatform with potential in the field of bio-photonic nanomedicine

Taojian Fan, Yansheng Zhou, Meng Qiu* and Han Zhang
*Shenzhen Engineering Laboratory of*
*Phosphorene and Optoelectronics*
*Key Laboratory of Optoelectronic Devices and*
*Systems of Ministry of Education*
*and Guangdong Province*
*College of Optoelectronic Engineering*
*Shenzhen University*
*Shenzhen 518060, P. R. China*
**qiumeng@szu.edu.cn*

Received 4 September 2018
Accepted 21 October 2018
Published 16 November 2018

Single- or few-layer black phosphorus (FLBP) has attracted great attentions in scientific community with its excellent properties, including biodegradability, unique puckered lattice configuration, attractive electrical properties and direct and tunable band gap. In recent years, FLBP has been widely studied in bio-photonic fields such as photothermal and photodynamic therapy, drug delivery, bioimaging and biosensor, showing attractive clinical potential. Because of the marked advantages of FLBP nanomaterials in bio-photonic fields, this review article reviews the latest advances of biomaterials based on FLBP in biomedical applications, ranging from biocompatibility, medical diagnosis to treatment.

*Keywords*: Black phosphorus; biosensing; drug delivery; biocompatibility; photothermal and photodynamic therapies.

## 1. Introduction

Two-dimensional (2D) materials, such as graphene,[1–9] transition metal dichalcogenides (TMDs, e.g., $MoS_2$,[10–19] $WS_2$,[20–25] $TiS_2$) and black phosphorus (BP), have been applied in various fields because of their distinctive physicochemical properties,[26–39] including easy surface modification, electrical conductivity and strong light response.[40–50] Especially, 2D materials own more advantages in bio-photonic applications such as biosensing,[51–61] cancer imaging[62–68]

*Corresponding author.

and drug delivery platform.[69–73] However, each 2D material has its own shortcoming which hinders its clinical applications.[74–77] Graphene displays an extremely high carrier mobility, but it has no bandgap,[78–88] which limits its applications in biosensing and bioimaging. In spite of possessing a finite bandgap,[17,89–96] the low carrier mobility of TMDs prevents their practical applications.[97–107] Taken together, it is important to find a new 2D material with a well-balanced performance.

BP is a novel nanoplatform with potential applications in such as energy storage,[35] sensor[108] and bio-photonic because of its excellent properties.[109–120] The bandgap of BP is tunable in a large range (from 0.3 eV to 2 eV) under different thicknesses.[121–124] As the result of the direct and tunable bandgap, few-layer black phosphorus (FLBP) processes a widely light absorption indicating a great potential in photothermal and photodynamic therapy. FLBP also shows high carrier mobility[125–130] while preserving large ON/OFF ratio.[131–137] Due to the balance of these features, BP is often occurred in biosensing and bioimaging field. FLBP, with the unique puckered lattice configuration, possesses much larger surface area-to-volume ratio than other 2D materials, which results in extremely high drug loading capacity.[138] Furthermore, FLBP displays negligible toxicity and outstanding biodegradability in the biological environment which distinguishes it from other common 2D materials. FLBP is completely degradable *in vivo*, and the products, such as phosphite ions, phosphate ions and other $P_xO_y$, are nontoxic and can be easily exhibited a desire renal filtration. In addition, FLBP possesses attractive electrical characteristics, unique band structure and natural biocompatibility, indicating that FLBP has a great potential for biomedical field.[37]

BP has aroused more and more research interest on its biomedicine applications with its unique physical and chemical properties. However, there is still a lot of problems needs to be solved to achieve the requirements of clinical applications, such as stability,[139–144] *in vivo* toxicity,[145] biodegradation,[146] excretion,[147] etc. In order to meet the urgent demand for the novel 2D materials used in biomedical field, it is necessary to summarize the latest achievement of BP in bio-photonic fields. In this paper, we mainly review the biomedical research of BP in biological diagnosis and therapy.

## 2. Biocompatibility of BP

Latiff *et al.*[145] established human lung carcinoma cancer epithelial cells (A549) model to study the toxicity of FLBP. To ensure the credibility of the results, graphene and $MoS_2$ are used as comparison and two similar methods based on similar principles were used to assess cell viabilities. In this work, the toxicity of FLBP increases with increasing concentration, when the concentration of FLBP is below 50 ppm. They found that toxicity of FLBP is lower than that of graphene but higher than that of $MoS_2$. Due to the limitations of the test method and the size of FLBP used in the paper, there are still a lot of toxicity assessments to do before the clinical applications of FLBP. Zhang *et al.*[148] studied the dependence of FLBP toxicity on size, concentration, exposure time and cell type, as presented in Fig. 1. FLBP was fabricated in oxygen-free Millipore water, and centrifugation at different speeds was used to obtain FLBP with three different sizes, named BP-1, BP-2 and BP-3, from large to small. The results of this paper indicate that FLBP with the BP-3 dimensions is appropriate for biomedical applications. They proposed and verified two possible mechanisms of the cytotoxicity of FLBP: (1) FLBP produces reactive oxygen species (ROS) to kill cells and (2) FLBP destroys cell membrane integrity. The cytotoxicity of BP-1 is much higher than that of BP-3. Fortunately, the size of BP-3 happens to be the most widely used size of FLBP nanosheets in the biomedical field. The results of this paper indicate that FLBP is appropriate for biomedical applications. Mu *et al.*[149] explored toxicological studies on BP quantum dots (BPQDs), which underwent faster renal filtration than BP nanosheets, systemically with cell and animal model. Comparing the cells viability and the endocellular ROS levels in experimental group with different concentrations of BPQDs and the control group, they found that the cytotoxicity of BPQDs is mainly derived from ROS produced by itself. The results of *in vivo* assays indicated that catalase activity in liver will reduce 24 h after injection, but there was no obvious adverse effect after a week without recurrence after a month. Song *et al.*[150] studied the dependence of FLBP cytotoxicity on dose and time. When the concentration exceeded 4 ppm, FLBP showed significant cytotoxicity, which conflicts with other works probably for the reason of the difference in the size of FLBP.

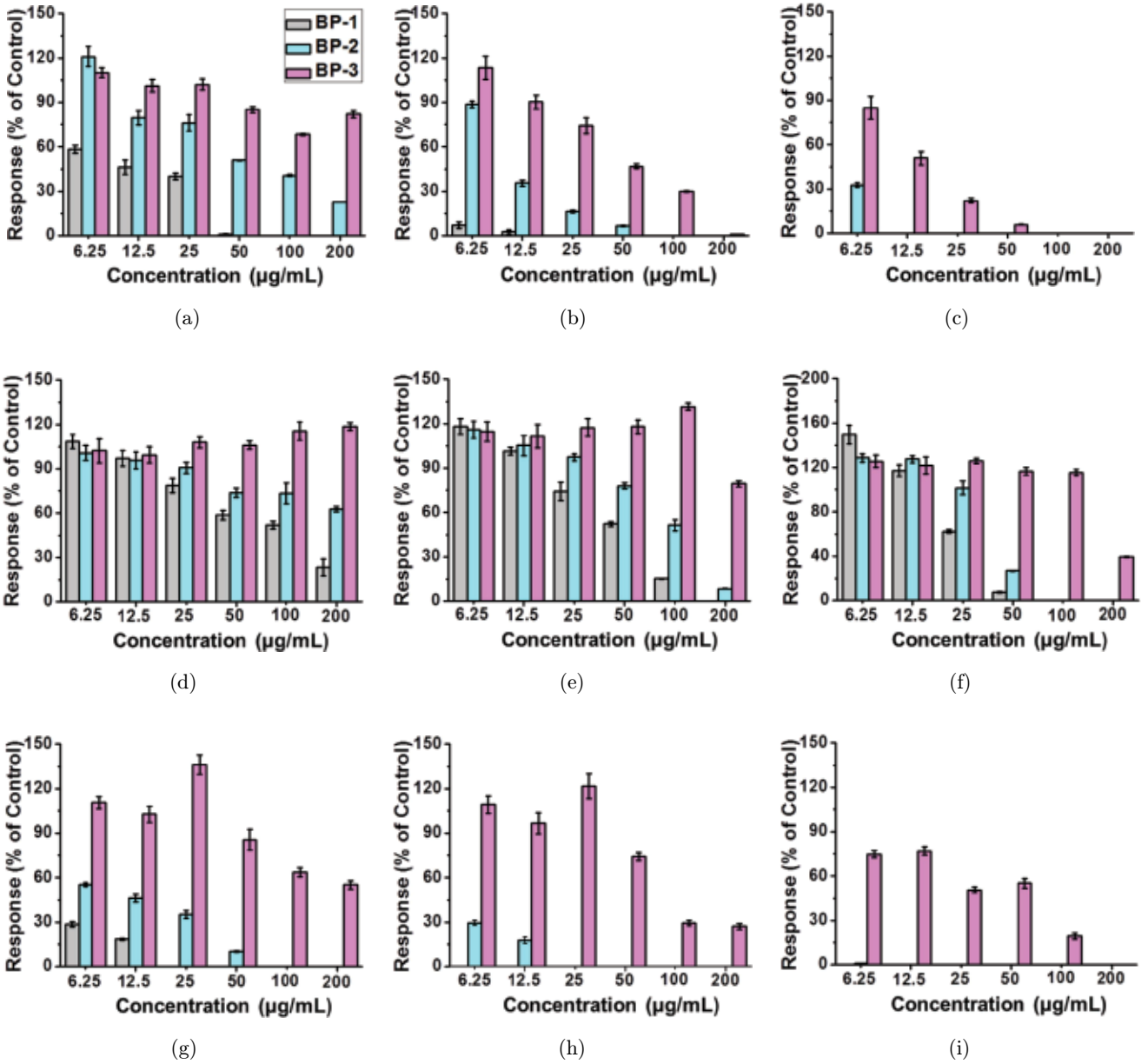


Fig. 1. The dependence of cell viability on size, concentration of BP, exposure time and cell lines. Cell lines: NIH 3T3 (a–c), HCoEpiC (d–f) and 293T cells (g–i). Exposure time: 12 h (a, d, g), 24 h (b, e, h) and 48 h (c, f, i).

The percentage of live cells was detected within 12 h at a dose of 10 ppm and was significantly reduced after 6 h, indicating the need for effective modification before BP achieves clinical applications.

## 3. Medical Diagnosis

### 3.1. *Biomolecular biosensors*

With a high carrier mobility and large switching ratios, FLBP has great applications potential on highly sensitive and selective biosensors.[151–160] Chen *et al.*[161] investigated FLBP for human immunoglobulin G (IgG) detection. FLBP was fabricated by a mechanical exfoliation method and passivated with $Al_2O_3$. The FLBP-based device showed rapid response performances and excellent sensitivity ($\sim$10 ng mL$^{-1}$) to human IgG. Furthermore, the FLBP-based device exhibited good stability without obvious changes in performance. Mayorga-Martinez *et al.*[162] obtained FLBP with the size of 40 $\sim$ 200 nm by electrochemical exfoliation. The as-fabricated FLBP showed active electrocatalytic performances for the hydrogen evolution

reaction and IgG detection. In addition, FLBP with poly-L-lysine (PLL) displays a great potential in label-free detection of myoglobin (Mb), which is an important signal of cardiovascular events.[163] FLBP was created by liquid-phase exfoliation (LPE) with an aqueous surfactant solution in argon atmosphere, and PLL was used to functionalize FLBP in order to accelerate binding with anti-Mb DNA aptamers. The PLL-BP dispersed stability in aqueous medium and showed a stable detection performance in phosphate-buffered saline (PBS) and serum samples, indicating successful surface modification. The FLBP-based device possesses a high sensitivity ($36\,\mu A\,pg^{-1}\,mL\,cm^{-2}$) and a low detection limit ($0.524\,pg\,mL^{-1}$), with a widely dynamic response range ($1\,pg\,mL^{-1}$ to $16\,\mu g\,mL^{-1}$).

In addition to excellent electrical properties, the unique fluorescence properties of FLBP were also applied to biological detection. Gu *et al.*[164] investigated BPQDs with a sonication-assisted solvothermal method for the applications of acetylcholinesterase activity sensing probes. The BPQDs showed strong green fluorescence at 497 nm and an extremely high quantum yield (8.4%). Furthermore, pH relevant fluorescence property with reliable photostability had been observed in this work. Lee *et al.*[165] prepared BPQDs with a strong visible blue-emitting performance by LPE in various organic solvents. They used catechol-grafted poly(ethylene glycol) (CA-PEG) to functionalize BPQDs in basic buffer to achieve a stable dispersible in water and an extremely low cytotoxicity. The photoluminescence emission centered of PEG-BPQDs is 428 nm and the photoluminescence quantum yield is ≈5% when the excitation wavelength is 365 nm. Yew *et al.*[166] demonstrated FLBP as a platform in fluorescence-based DNA biosensors. BP crystals transformed from red phosphorus allotrope in the high pressure, and FLBP was synthesized by share force milling at 17,000 rpm. FLBP showed an obvious photoluminescence emission centered at 527 nm with an excitation wavelength of 200 nm, indicating potential applications as fluorescent sensing platform. This biosensor shows a low detection limit (5.9 pM) and quantification limit (19.7 pM). In addition, an excellent linearity ($r = 0.91$) and a widely dynamic response range (4–4000 pM) were observed in this work.

### 3.2. *Tumor imaging*

Cancer is a malignant disease that kills millions of people every year.[38,167–177] With the enhanced permeability and retention (EPR) effect,[178–188] FLBP can be passively enriched to the tumor site, so the tumor imaging based on FLBP has received extensive attention. Shao *et al.*[147] investigated that BPQDs, which manufactured by the simple liquid exfoliation method, with poly lactic-co-glycolic acid (PLGA) were used to modify BPQDs in order to enhance the stability and solubility of BPQDs in water. As-fabricated BP-PLGA can effectively passively accumulate to the tumor region with tail vein injection because of the EPR effect. Figure 2(a) demonstrates the infrared thermographic images of the mice irradiated by near-infrared (NIR) laser 24 h after injection. Drawing a comparison between the tumor temperature of the test groups and of the control groups under the same power irradiation, it is obvious that the tumor temperature of the test groups (26.3°C of BP-PLGA) increased much more than that of the control groups (6.2°C, 7.8°C and 10.8°C of PBS, PLGA and bare BPQDs, respectively), indicating the excellent photothermal performance of BP-PLGA. In addition, many other researchers also have achieved extremely good photothermal imaging by different modifications of FLBP.[189,190]

Sun *et al.*[191] investigated BPQDs with excellent photostability for the applications of photoacoustic (PA) imaging, as shown in Fig. 2(b). The PEGylated BPQDs with a uniform size were fabricated by a simple high energy mechanical milling method. When the concentration of the PEGylated BPQDs is in the range of 0–250 $\mu g\,mL^{-1}$, the intensity of the PA signal rises linearly as the concentration increases. Furthermore, the PA signal intensity in tumor was still higher than that of liver and kidney, 24 h after injection, representing a long retention time and EPR effect. Sun *et al.*[192] reported BPQDs loaded with titanium ligand (TiL4) as PA imaging agent. Dispersibility and stability of $TiL_4$@BPQDs in water are much better than those of bare BPQDs. With increasing wavelength of the irradiation, the intensity of the PA signal decreased because the optical absorption of wavelength range from 680 nm to 808 nm reduces.

Yang *et al.*[193] prepared FLBP coated with Au nanoparticles for surface-enhanced Raman scattering (SERS) imaging. BP–Au NSs were fabricated with a facile reflux method, and mPEG-SH was added to improve the dispersion and stability in water. The molecular mechanism of photothermal therapy (PTT) was investigated by SERS analysis.

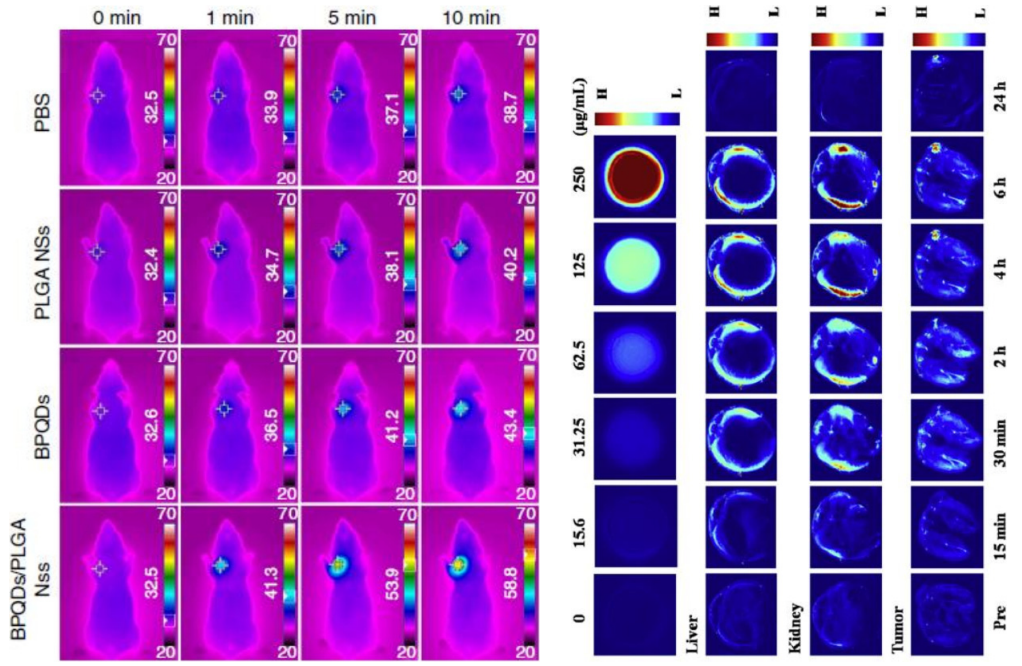


(a) (b)

Fig. 2. (a) Infrared thermographic images in the nude mice bearing MCF7 breast tumor under NIR laser irradiation (808 nm, 1 W cm$^{-2}$) after intravenous injection at 24 h with different treatments. (b) PA maps of PEGylated BP nanoparticles dispersions with different concentrations (first column), and time-lapsed PA images of liver, kidney and tumor of female BALB/c mice after intravenous injection with PEGylated BP nanoparticles (200 mL, 2 mg mL$^{-1}$).

The SERS analysis illustrates that PTT damages the membrane microstructure in tumor, and some BP–Au NSs appear in the nucleus region.

## 4. Medical Therapy

### 4.1. *Phototherapy*

Phototherapy, mainly including PTT[194,195] and photodynamic therapeutic (PDT),[196,197] has become a potential alternative to traditional cancer therapy with its advantages of little double consequences,[198–205] excellent targeting[206–215] and intelligent controllability.[216–222] The principle of PTT is based on the heat energy generated by the photothermal agent under irradiation to achieve the therapeutic effect. PDT agent can generate ROS to kill cancer cells under laser irradiation. FLBP has broadband absorption characteristics because of its tunable direct band gap, indicating great potential for the applications of cancer phototherapy.

#### 4.1.1. *PTT*

Sun *et al.*[223] fabricated BPQDs by liquid exfoliation method as photothermal agent. BPQDs were functionalized with PEG to prevent BPQDs from aggregating in PBS. As-fabricated PEG-BPQDs possessed a large extinction coefficient (14.8 L g$^{-1}$ cm$^{-1}$ at 808 nm), which is much more larger than that of Au nanorods. In addition, PEG-BPQDs showed a high photothermal conversion efficiency (28.4%) and favorable photostability. The aqueous solutions of PEG-BPQDs rise 31.5°C in 10 min at the concentration of 50 ppm when the power density of NIR laser irradiation is 1.0 W cm$^{-2}$, indicating an excellent photothermal performance. The percentage of live cells had no significant decrease even with a high incubation concentration of PEG-BPQDs (200 ppm) without NIR laser. The PEG-BPQDs killed the most of the cancer cells with a low concentration after the NIR irradiation for 10 min, as shown in Fig. 3. The results of this work illustrate the good biocompatibility and photothermal performance of BPQDs.

Shao *et al.*[147] demonstrated BPQDs coated with PLGA for PTT. PLGA enhanced the stability of BPQDs and adjusted the degradation rate of nanoparticles by adjusting the chemical composition. PLGA-BPQDs maintained stable photothermal properties within 8 days, and it degraded by almost 80% after 8 weeks, indicating a balance of

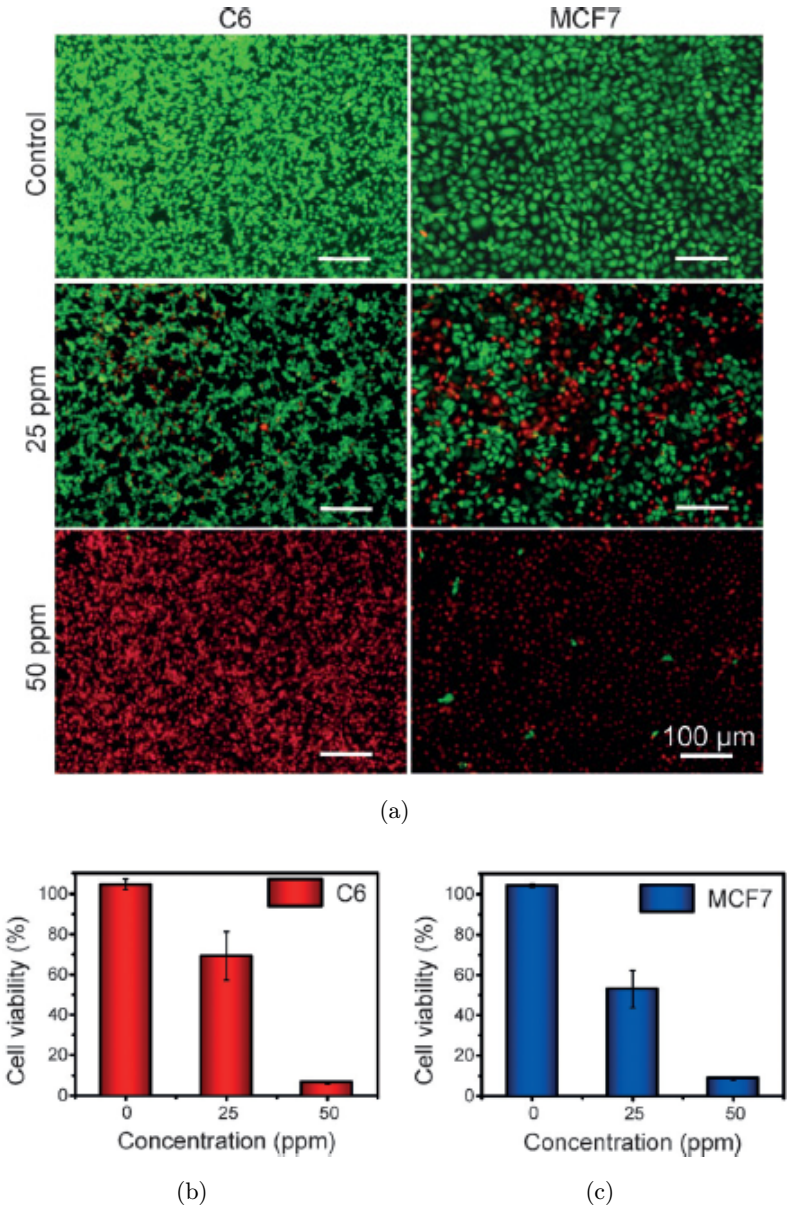


Fig. 3. The dependence of cell viability on concentration of BPQDs and cell lines. The irradiation time is 10 min and power density of 808 nm laser is 1.0 W cm$^{-2}$. (a) Fluorescence images of cancer cells incubated with BPQDs after irradiation of 808 nm laser. (b) C6 cells viability after treatments with different concentrations of BPQDs. (c) MCF7 cells viability after treatments with different concentrations of BPQDs.

therapeutic and biodegradable. *In vitro* experiments showed that PLGA-BPQDs killed the most of cancer cells at an extremely low concentration (10 ppm). What's more, the final degradation products of PLGA-BPQDs are carbon dioxide, water, phosphate and phosphonate, which normally exist both *in vivo* and *in vitro* and result in little side effects. Fu *et al.*[224] prepared three types of FLBP with average size of $394 \pm 75$ nm, $118 \pm 22$ nm and $4.5 \pm 0.6$ nm by LPE method, named as L-BP, M-BP and S-BP. The temperature of L-BP solution with a concentration of 25 ppm was able to rise by 24°C under NIR laser irradiation for 10 min, whereas temperatures of M-BP and S-BP solutions with the equal concentration could only rise by 21.8°C and 19.2°C, indicating that L-BP has the best photothermal performance. In addition, there are some studies dedicated to improving the photothermal stability of FLBP.[225–227] Some researchers explored new applications for the thermal performance of BP, such as post-surgical treatment of cancer, 3D-printed scaffolds and neuroprotective nanomedicine.[189,228,229]

#### 4.1.2. *PDT*

FLBP for PDT was fabricated by LPE in an aqueous solvent.[230] At a wavelength of 530 nm, the quantum yield of FLBP producing singlet oxygen is very high (0.91). *In vitro* and *in vivo* FLBP experiments showed good PDT effects, as shown in Fig. 4. BPQDs were synthesized by LPE in *N*-methyl pyrrolidone and coated with PEG to achieve enhanced stability in water. Guo *et al.*[231] used BP dispersion to incubate cancer cells under 670 nm laser irradiation and researched the dependence of cell survival rate on BPQD concentrations, illumination time and laser intensity. The ROS generated by FLBP was able to kill the cancer cells efficiently at very low concentration (1.6 ppm) and at very weak laser power (160 mW cm$^{-2}$). Furthermore, 65% of BPQDs was found excreted with urine within 8 h, probably for the reason of the ultra-small hydrodynamic size of BPQDs, indicating that BPQDs have a good biocompatibility. Chen *et al.*[232] found that the bleaching signal of BPQDs is built up rapidly (<2 ns) and lasts a long time (100 $\mu$s).

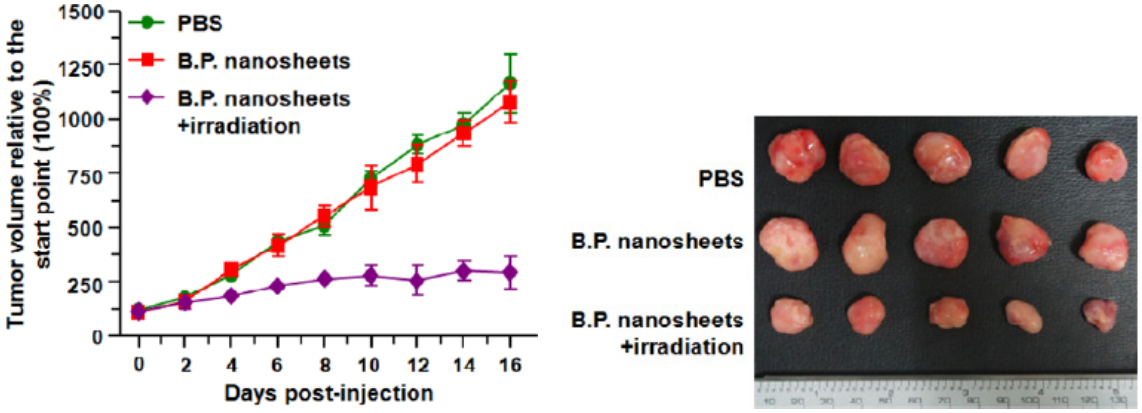


(a) (b)

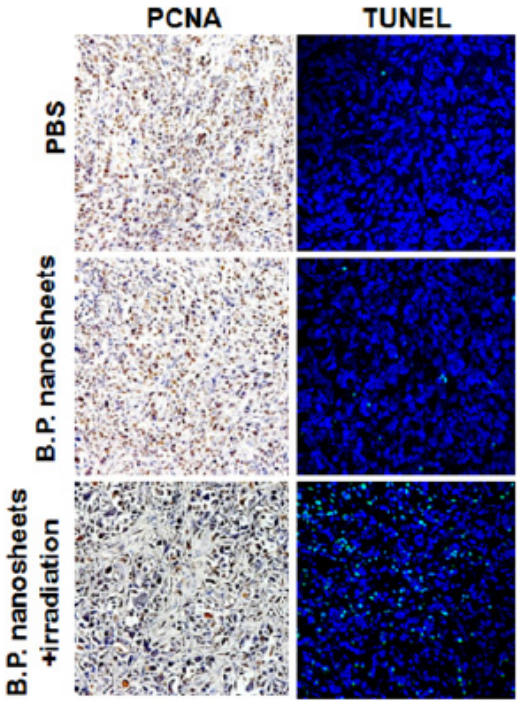


(c)

Fig. 4. *In vivo* PDT. (a) Tumor volume of different time post-injections. (b) Tumor pictures of experimental group and control group after treatments. (c) PCNA and TUNEL analysis of tumor tissues.

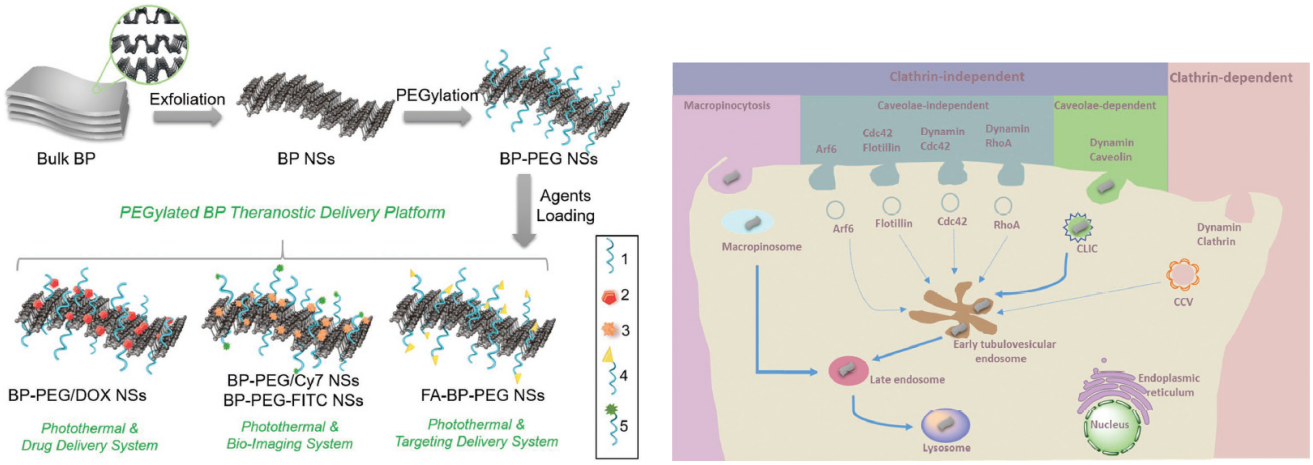


(a) (b)

Fig. 5. (a) Schematic representation of the FLBP nanoparticle. 1: PEG-NH2 (surface modification), 2: DOX (therapeutic agents), 3: Cy7-NH2 (NIR imaging agents), 4: FA-PEG-NH2 (targeting agents), 5: FITC-PEG-NH2 (fluorescent imaging agents). (b) The endocytosis pathway of the FLBP nanoparticle.

The triplet generation attributed to intersystem crossing was observed and may be the reason of the highly efficient singlet oxygen generation of BPQDs. Tan *et al.*[233] achieved *in situ* disinfection with PDT based on FLBP. FLBP was modified with poly(4-pyridonemethylstyrene) endoperoxide (PPMS-EPO). PPMS not only enhances the stability of FLBP, but also stores singlet oxygen. The PPMS-EPO/BPS showed good photodynamic performance even in the absence of light, indicating a good clinical potential.

### 4.2. *Therapeutic agent delivery*

Chemotherapy is an effective cancer treatment,[234,235] but the high toxicity,[236] low targeting[237,238] and drug resistance[239] limit its therapeutic effect. In order to solve the aforementioned problems, researchers load therapeutic agents onto drug delivery systems (DDSs) to enhance chemotherapeutic effect. With large surface area-to-volume radio, unique pleated structure and excellent light response characteristics, FLBP has great potential for DDSs. Tao *et al.*[240] first applied FLBP to DDSs, as shown in Fig. 5. PEG-FA/Cy7-functionalized FLBP exhibited good biocompatibility, obvious tumor targeting and strong fluorescence signal and was loaded with doxorubicin (DOX) via electrostatic adsorption. In addition, the endocytosis pathway of the FLBP nanoparticle had also been screened. Chen *et al.*[138] prepared a drug loading platform with a pH/photo response based on FLBP. Their results showed that FLBP has a very high DOX loading (980%) due to its puckered lattice configuration, large interlay distance 0.524 nm and negative charge. They used the therapeutic system to achieve synergistic treatment of PTT/PDT/chemotherapy and achieved good anti-tumor effects. Wang *et al.*[241] used one-pot method to prepare HSA-modified FLBP, which can effectively load paclitaxel by hydrophobic interactions. Qiu *et al.*[190] fabricated a BP@hydrogel-based DDS. The DDSs enable intelligent light-controlled drug release and degradation, and the degradation products are completely nontoxic and easily metabolized. Yin *et al.*[242] fabricated FLBP loaded with interfering RNA as the applications of gene delivery systems. Compared with the commercial delivery reagents, the BPQDs exhibited a higher transfection efficiency and low toxicity.

## 5. Summary

This paper summarizes the latest progress in FLBP research from three aspects, including biocompatibility of BP, medical diagnosis and medical therapeutic based on BP. Various factors such as size, concentration and test cell line can affect the toxicity of FLBP, but overall, FLBP shows relatively low toxic at effective dosing dose. Due to its attractive electrical properties, fluorescence characteristics and large surface area-to-volume

ratio, FLBP shows a great potential for biosensors and imaging. In terms of biological therapy, FLBP mainly achieves therapeutic effects through its excellent optical response characteristics and as a drug delivery platform.

Although studies on the biomedical applications of FLBP have made a lot of progress, there are still some problems that need to be solved before its clinical translation. First of all, because the size of the FLBP has a great impact on toxicity and treatment effects, it is very important to find a novel method to fabricate FLBP with uniform size and high production. Secondly, other treatments such as chemotherapy, immunotherapy, etc. could be combined with BP to achieve synergistic effect. Finally, the targeted treatments based on FLBP should be developed for specific diseases to achieve smaller side effects and better therapeutic effects. This requires multidisciplinary researchers to work together. FLBP has great potential in biomedicine. To promote the clinical applications of FLBP, we summarized the progress of FLBP in biomedical field.

## Abbreviations

| | |
|---|---|
| FLBP | few-layer black phosphorus |
| 2D | two-dimensional |
| BP | black phosphorus |
| TMDs | transition metal dichalcogenides |
| ROS | reactive oxygen species |
| QDs | quantum dots |
| IgG | immunoglobulin G |
| PLL | poly-L-lysine |
| Mb | myoglobin |
| PBS | Phosphate-buffered saline |
| CA-PEG | catechol-grafted poly (ethylene glycol) |
| EPR | enhanced permeability and retention |
| PLGA | poly lactic-co-glycolic acid |
| NIR | near-infrared |
| PA | Photoacoustic |
| HEMM | high energy mechanical milling |
| TiL4 | titanium ligand |
| SERS | surface-enhanced Raman scattering |
| PTT | photothermal therapy |
| PDT | photodynamic therapeutic |
| PEG | poly (ethylene glycol) |
| NMP | *N*-methyl pyrrolidone |
| PPMS-EPO | poly(4-pyridonemethylstyrene) endoperoxide |
| DDSs | drug delivery systems |
| DOX | Doxorubicin |

## Acknowledgments

We acknowledge financial support from the National Natural Science Foundation of China (61435010 and 61575089, H. Z.), the Science and Technology Innovation Commission of Shenzhen (KQTD-2015032416270385 and JCYJ20150625103619275, H. Z.), the China Postdoctoral Science Foundation (2017M610540, 2018T110892, M. Q.), the Natural Science Foundation of Shandong Province, China (ZR2016BB33, M. Q.) and the Natural Science Foundation of Guangdong Province, China (2018A030310500, M. Q.).

## References

1. A. R. Akhmerov, C. W. J. Beenakker, "Boundary conditions for Dirac fermions on a terminated honeycomb lattice," *Physics* **77**, 439–446 (2008).
2. D. M. Basko, "Boundary problems for Dirac electrons and edge-assisted Raman scattering in graphene," *Phys. Rev. B Condens. Matter* **79**, 205428 (2009).
3. W. Beugeling, J. C. Everts, C. M. Smith, "Topological phase transitions driven by next-nearest-neighbor hopping in two-dimensional lattices," *Phys. Rev. B* **86**, 1721–1725 (2012).
4. K. I. Bolotin, K. J. Sikes, Z. Jiang, M. Klima, G. Fudenberg, J. Hone, P. Kim, H. L. Stormer, "Ultrahigh electron mobility in suspended graphene," *Solid State Commun.* **146**, 351–355 (2008).
5. A. Girit, J. C. Meyer, R. Erni, M. D. Rossell, C. Kisielowski, Y. Li, C. H. Park, M. F. Crommie, M. L. Cohen, S. G. Louie, "Graphene at the edge: Stability and dynamics," *Science* **323**, 1705–1708 (2009).
6. X. Li, D. Geng, Y. Zhang, X. Meng, R. Li, X. Sun, "Superior cycle stability of nitrogen-doped graphene nanosheets as anodes for lithium ion batteries," *Electrochem. Commun.* **13**, 822–825 (2011).
7. B. Shen, J. Chen, X. Yan, Q. Xue, "Synthesis of fluorine-doped multi-layered graphene sheets by arc-discharge," *Rsc Adv.* **2**, 6761–6764 (2012).
8. H. W. Yoon, Y. H. Cho, H. B. Park, "Graphene-based membranes: Status and prospects," *Philos. Trans.* **374**, 20150024 (2016).
9. J. Zhang, Z. Xie, W. Li, S. Dong, M. Qu, "High-capacity graphene oxide/graphite/carbon nanotube

composites for use in Li-ion battery anodes," *Carbon* **74**, 153–162 (2014).
10. S. De Jong, A. Haas, J. Qian, G. Blazey, D. Hedin, A. Sanchezhernandez, A. Heinson, J. G. Lima, R. Madaras, A. Duperrin, "Atomically thin MoS2: A new direct-gap semiconductor," *Phys. Rev. Lett.* **105**, 136805 (2010).
11. G. Eda, H. Yamaguchi, D. Voiry, T. Fujita, M. Chen, M. Chhowalla, "Photoluminescence from chemically exfoliated MoS2," *Nano Lett.* **11**, 5111–5116 (2011).
12. Q. He, Z. Zeng, Z. Yin, H. Li, S. Wu, X. Huang, H. Zhang, "Fabrication of flexible MoS2 thin–film transistor arrays for practical gas–sensing applications," *Small* **8**, 2994–2999 (2012).
13. D. Jariwala, V. K. Sangwan, D. J. Late, J. E. Johns, V. P. Dravid, T. J. Marks, L. J. Lauhon, M. C. Hersam, "Band-like transport in high mobility unencapsulated single-layer MoS2 transistors," *Appl. Phys. Lett.* **102**, 699 (2013).
14. J. Liu, Z. Zeng, X. Cao, G. Lu, L. H. Wang, Q. L. Fan, W. Huang, H. Zhang, "Preparation of MoSâ,-polyvinylpyrrolidone nanocomposites for flexible nonvolatile rewritable memory devices with reduced graphene oxide electrodes," *Small* **8**, 3517–3522 (2012).
15. B. Radisavljevic, A. Radenovic, J. Brivio, V. Giacometti, A. Kis, "Single-layer MoS2 transistors," *Nat. Nanotechnol.* **6**, 147–150 (2011).
16. B. Radisavljevic, M. B. Whitwick, A. Kis, "Integrated circuits and logic operations based on single-layer MoS2," *ACS Nano* **5**, 9934–9938 (2011).
17. A. Splendiani, L. Sun, Y. Zhang, T. Li, J. Kim, C. Y. Chim, G. Galli, F. Wang, "Emerging photoluminescence in monolayer MoS2," *Nano Lett.* **10**, 1271–1275 (2010).
18. H. Wang, L. Yu, Y. H. Lee, Y. Shi, A. Hsu, M. L. Chin, L. J. Li, M. Dubey, J. Kong, T. Palacios, "Integrated circuits based on bilayer MoS2 transistors," *Nano Lett.* **12**, 4674 (2012).
19. Z. Yin, H. Li, H. Li, L. Jiang, Y. Shi, Y. Sun, G. Lu, Q. Zhang, X. Chen, H. Zhang, "Single-layer MoS2 phototransistors," *ACS Nano* **6**, 74–80 (2012).
20. C. Cong, J. Shang, X. Wu, B. Cao, N. Peimyoo, C. Qiu, L. Sun, T. Yu, "Synthesis and optical properties of large area single crystalline 2D semiconductor WS2 monolayer from chemical vapor deposition," *Adv. Opt. Mater.* **2**, 131–136 (2014).
21. A. L. Elías, N. Perealópez, A. Castrobeltrán, A. Berkdemir, R. Lv, S. Feng, A. D. Long, T. Hayashi, Y. A. Kim, M. Endo, "Controlled synthesis and transfer of large-area WS2 sheets: From single layer to few layers," *ACS Nano* **7**, 5235–5242 (2013).
22. K. M. Mccreary, A. T. Hanbicki, S. Simranjeet, R. K. Kawakami, G. G. Jernigan, I. Masa, N. Amy, T. H. Brintlinger, R. M. Stroud, B. T. Jonker, "The effect of preparation conditions on Raman and photoluminescence of monolayer WS2," *Sci. Rep.* **6**, 35154 (2016).
23. M. Okada, T. Sawazaki, K. Watanabe, T. Taniguch, H. Hibino, H. Shinohara, R. Kitaura, "Direct chemical vapor deposition growth of WS2 atomic layers on hexagonal boron nitride," *ACS Nano* **8**, 8273–8277 (2014).
24. N. Peimyoo, J. Shang, C. Cong, X. Shen, X. Wu, E. K. Yeow, T. Yu, "Nonblinking, intense two-dimensional light emitter: Monolayer WS2 triangles," *ACS Nano* **7**, 10985–10994 (2013).
25. Y. Zhang, Y. Zhang, Q. Ji, J. Ju, H. Yuan, J. Shi, T. Gao, D. Ma, M. Liu, Y. Chen, "Controlled growth of high-quality monolayer WS2 layers on sapphire and imaging its grain boundary," *ACS Nano* **7**, 8963–8971 (2013).
26. H. Huang, M. Qiu, Q. Li, S. Liu, X. Zhang, Z. Wang, N. Fu, B. Zhao, R. Yang, W. Huang, "Donor–acceptor conjugated polymers based on thieno[3,2-b]indole (TI) and 2,1,3-benzothiadiazole (BT) for high efficiency polymer solar cells," *J. Mater. Chem. C* **4**, 5448–5460 (2016).
27. S. Han, D. Wu, S. Li, F. Zhang, X. Feng, "ChemInform abstract: Porous graphene materials for advanced electrochemical energy storage and conversion devices," *Adv. Mater.* **26**, 849–864 (2014).
28. Z. Jiang, B. Pei, A. Manthiram, "Randomly stacked holey graphene anodes for lithium ion batteries with enhanced electrochemical performance," *J. Mater. Chem. A* **1**, 7775–7781 (2013).
29. M. Qiu, S. Long, B. Li, L. Yan, W. Xie, Y. Niu, X. Wang, Q. Guo, A. Xia, "Toward an understanding of how the optical property of water-soluble cationic polythiophene derivative is altered by the addition of salts: The Hofmeister effect," *J. Phys. Chem. C* **117**, 21870–21878 (2013).
30. W. C. Ren, L. B. Gao, L. P. Ma, H. M. Cheng, "Preparation of graphene by chemical vapor deposition," *Carbon* **49**, 2881 (2011).
31. D. Zhu, Q. Zhu, C. Gu, D. Ouyang, M. Qiu, X. Bao, R. Yang, "Alkoxyl side chain substituted thieno[3,4-c]pyrrole-4,6-dione to enhance photovoltaic performance with low steric hindrance and high dipole moment," *Macromolecules* **49**, 5788–5795 (2016).
32. M. Qiu, D. Zhu, X. Bao, J. Wang, X. Wang, R. Yang, "WO3 with surface oxygen vacancies as an anode buffer layer for high performance polymer solar cells," *J. Mater. Chem. A* **4**, 894–900 (2016).
33. M. Qiu, D. Zhu, L. Yan, N. Wang, L. Han, X. Bao, Z. Du, Y. Niu, R. Yang, "Strategy to manipulate

molecular orientation and charge mobility in D-A type conjugated polymer through rational fluorination for improvements of photovoltaic performances," *J. Phys. Chem. C* **120**, 22757–22765 (2016).

34. M. Qiu, R. G. Brandt, Y. Niu, X. Bao, D. Yu, N. Wang, L. Han, L. Yu, S. Xia, R. Yang, "Theoretical study on the rational design of cyano-substituted P3HT materials for OSCs: Substitution effect on the improvement of photovoltaic performance," *J. Phys. Chem. C* **119**, 8501–8511 (2015).
35. Y. Zhang, Y. Zheng, K. Rui, H. H. Hng, K. Hippalgaonkar, J. Xu, W. Sun, J. Zhu, Q. Yan, W. Huang, "2D black phosphorus for energy storage and thermoelectric applications," *Small* **13**, 1700661 (2017).
36. W. Lei, G. Liu, J. Zhang, M. Liu, "Black phosphorus nanostructures: Recent advances in hybridization, doping and functionalization," *Chem. Soc. Rev.* **46**, 3492 (2017).
37. M. Qiu, W. X. Ren, T. Jeong, M. Won, G. Y. Park, D. K. Sang, L.-P. Liu, H. Zhang, J. S. Kim, "Omnipotent phosphorene: A next-generation, two-dimensional nanoplatform for multidisciplinary biomedical applications," *Chem. Soc. Rev.* **47**, 5588–5601 (2018).
38. Y. Lin, Y. Wu, R. Wang, G. Tao, P. F. Luo, X. Lin, G. Huang, J. Li, H. H. Yang, "Two-dimensional tellurium nanosheets for photoacoustic imaging-guided photodynamic therapy," *Chem. Commun.* **54**, 8579–8582 (2018).
39. T. Guo, Y. Lin, Z. Li, S. Chen, G. Huang, H. Lin, J. Wang, G. Liu, H. H. Yang, "Gadolinium oxysulfide-coated gold nanorods with improved stability and dual-modal magnetic resonance/photoacoustic imaging contrast enhancement for cancer theranostics," *Nanoscale* **9**, 56–61 (2017).
40. Z. Chen, X. Liu, Y. Liu, S. Gunsel, J. Luo, "Ultrathin MoS2 nanosheets with superior extreme pressure property as boundary lubricants," *Sci. Rep.* **5**, 12869 (2015).
41. L. Cizaire, B. Vacher, T. L. Mogne, J. M. Martin, L. Rapoport, A. Margolin, R. Tenne, "Mechanisms of ultra-low friction by hollow inorganic fullerene-like MoS 2 nanoparticles," *Surf. Coat. Technol.* **160**, 282–287 (2002).
42. J. J. Hu, J. E. Bultman, J. S. Zabinski, "Microstructure and lubrication mechanism of multilayered MoS 2/Sb 2 O 3 thin films," *Tribol. Lett.* **21**, 169–174 (2006).
43. B. Huard, N. Stander, J. A. Sulpizio, D. Goldhaber-Gordon, "Evidence of the role of contacts on the observed electron-hole asymmetry in graphene," *Phys. Rev. B* **78**, 121402 (2008).
44. W. J. Liu, H. Y. Yu, J. Wei, M. F. Li, "Impact of process induced defects on the contact characteristics of Ti/graphene devices," *Electrochem. Solid-State Lett.* **14**, K67 (2011).
45. K. Nagashio, T. Nishimura, K. Kita, A. Toriumi, "Contact resistivity and current flow path at metal/graphene contact," *Appl. Phys. Lett.* **97**, 1068 (2010).
46. T. Xian, W. Liang, J. Zhao, Z. Li, Q. Meng, T. Fan, C. S. Luo, Z. Ye, L. Yu, Z. Guo, "Fluorinated phosphorene: Electrochemical synthesis, atomistic fluorination, and enhanced stability," *Small* **13**, 1702739 (2017).
47. Z. Xie, D. Wang, T. Fan, C. Xing, Z. Li, W. Tao, L. Liu, S. Bao, D. Fan, H. Zhang, "Black phosphorus analogue tin sulfide nanosheets: Synthesis and application as near-infrared photothermal agents and drug delivery platforms for cancer therapy," *J. Mater. Chem. B* **6**, 4747–4755 (2018).
48. C. Xing, W. Huang, Z. Xie, J. Zhao, D. Ma, T. Fan, W. Liang, Y. Ge, B. Dong, J. Li, "Ultra-small bismuth quantum dots: Facile liquid-phase exfoliation, characterization, and application in high-performance UV-Vis photo-detector," *ACS Photon.* **5**, 621–629 (2017).
49. Y. Song, Z. Liang, X. Jiang, Y. Chen, Z. Li, L. Lu, Y. Ge, K. Wang, J. Zheng, S. Lu, "Few-layer antimonene decorated microfiber: Ultra-short pulse generation and all-optical thresholding with enhanced long term stability," *2d Mater.* **4**, 045010 (2017).
50. Y. Ge, Z. Zhu, Y. Xu, Y. Chen, S. Chen, Z. Liang, Y. Song, Y. Zou, H. Zeng, S. Xu, "Ultrafast photonics: Broadband nonlinear photoresponse of 2D TiS2 for ultrashort pulse generation and alloptical thresholding devices (Advanced Optical Materials 4/2018)," *Adv. Opt. Mater.* **6**, 1870014 (2018).
51. H. Dong, J. Zhang, H. Ju, H. Lu, S. Wang, S. Jin, K. Hao, H. Du, X. Zhang, "Highly sensitive multiple microRNA detection based on fluorescence quenching of graphene oxide and isothermal strand-displacement polymerase reaction," *Anal. Chem.* **84**, 4587–4593 (2012).
52. P. Hu, C. Zhu, L. Jin, S. Dong, "An ultrasensitive fluorescent aptasensor for adenosine detection based on exonuclease III assisted signal amplification," *Biosens. Bioelectron.* **34**, 83–87 (2012).
53. B. Li, X. Li, M. Wang, Z. Yang, H. Yin, S. Ai, "Photoelectrochemical biosensor for highly sensitive detection of microRNA based on duplex-specific nuclease-triggered signal amplification," *J. Solid State Electrochem.* **19**, 1301–1309 (2015).
54. Y. Lu, P. Wu, Y. Yin, H. Zhang, C. Cai, "Aptamer-functionalized graphene oxide for highly efficient loading and cancer cell-specific delivery of antitumor drug," *J. Mater. Chem. B* **2**, 3849–3859 (2014).

55. Y. Ohno, K. Maehashi, K. Matsumoto, "Label-free biosensors based on aptamer-modified graphene field-effect transistors," *J. Am. Chem. Soc.* **132**, 18012–18013 (2010).
56. J. Z. Ou, A. F. Chrimes, Y. Wang, S. Y. Tang, M. S. Strano, K. Kalantarzadeh, "Ion-driven photoluminescence modulation of quasi-two-dimensional MoS2 nanoflakes for applications in biological systems," *Nano Lett.* **14**, 857 (2014).
57. D. Sarkar, W. Liu, X. Xie, A. C. Anselmo, S. Mitragotri, K. Banerjee, "MoS2 field-effect transistor for next-generation label-free biosensors," *ACS Nano* **8**, 3992 (2014).
58. P. Wu, Y. Qian, P. Du, H. Zhang, C. Cai, "Facile synthesis of nitrogen-doped graphene for measuring the releasing process of hydrogen peroxide from living cells," *J. Mater. Chem.* **22**, 6402–6412 (2012).
59. Q. Xi, D. M. Zhou, Y. Y. Kan, J. Ge, Z. K. Wu, R. Q. Yu, J. H. Jiang, "Highly sensitive and selective strategy for microRNA detection based on WS2 nanosheet mediated fluorescence quenching and duplex-specific nuclease signal amplification," *Anal. Chem.* **86**, 1361 (2014).
60. X. H. Zhao, Q. J. Ma, X. X. Wu, X. Zhu, "Graphene oxide-based biosensor for sensitive fluorescence detection of DNA based on exonuclease III-aided signal amplification," *Anal. Chim. Acta* **727**, 67–70 (2012).
61. C. Zhu, Z. Zeng, H. Li, F. Li, C. Fan, H. Zhang, "Single-layer MoS2-based nanoprobes for homogeneous detection of biomolecules," *J. Am. Chem. Soc.* **135**, 5998 (2013).
62. L. Cheng, J. Liu, X. Gu, H. Gong, X. Shi, T. Liu, C. Wang, X. Wang, G. Liu, H. Xing, "PEGylated WS(2) nanosheets as a multifunctional theranostic agent for *in vivo* dual-modal CT/photoacoustic imaging guided photothermal therapy," *Adv. Mater.* **26**, 1886–1893 (2014).
63. T. Liu, S. Shi, C. Liang, S. Shen, L. Cheng, C. Wang, X. Song, S. Goel, T. E. Barnhart, W. Cai, "Iron oxide decorated MoS2 nanosheets with double PEGylation for chelator-free radiolabeling and multimodal imaging guided photothermal therapy," *ACS Nano* **9**, 950–960 (2015).
64. T. Liu, C. Wang, W. Cui, H. Gong, C. Liang, X. Shi, Z. Li, B. Sun, Z. Liu, "Combined photothermal and photodynamic therapy delivered by PEGylated MoS2 nanosheets," *Nanoscale* **6**, 11219–11225 (2014).
65. X. Qian, S. Shen, T. Liu, L. Cheng, Z. Liu, "Two-dimensional TiSâ, nanosheets for *in vivo* photoacoustic imaging and photothermal cancer therapy," *Nanoscale* **7**, 6380–6387 (2015).
66. L. V. Wang, S. Hu, "Photoacoustic tomography: *In vivo* imaging from organelles to organs," *Science* **335**, 1458–1462 (2012).
67. S. Wang, X. Li, Y. Chen, X. Cai, H. Yao, W. Gao, Y. Zheng, X. An, J. Shi, H. Chen, "A facile one-pot synthesis of a two-dimensional MoS2/Bi2 S3 composite theranostic nanosystem for multi-modality tumor imaging and therapy," *Adv. Mater.* **27**, 2775–2782 (2015).
68. Y. Yong, L. Zhou, Z. Gu, L. Yan, G. Tian, X. Zheng, X. Liu, X. Zhang, J. Shi, W. Cong, "WS2 nanosheet as a new photosensitizer carrier for combined photodynamic and photothermal therapy of cancer cells," *Nanoscale* **6**, 10394–10403 (2014).
69. W. Tao, X. Ji, X. Xu, M. A. Islam, Z. Li, S. Chen, P. E. Saw, H. Zhang, Z. Bharwani, Z. Guo, "Inside cover: Antimonene quantum dots: Synthesis and application as near infrared photothermal agents for effective cancer therapy (*Angew. Chem. Int. Ed.* 39/2017)," *Angew. Chem.* **56**, 11896 (2017).
70. T. Liu, C. Wang, X. Gu, H. Gong, L. Cheng, X. Shi, L. Feng, B. Sun, Z. Liu, "Drug delivery with PEGylated MoS2 nano-sheets for combined photothermal and chemotherapy of cancer," *Adv. Mater.* **26**, 3433–3440 (2014).
71. Y. Ma, H. Wang, Y. Dan, Y. Wei, Y. Cao, P. Yi, H. Zhang, Z. Deng, J. Dai, X. Liu, "Magnetic resonance imaging revealed splenic targeting of canine parvovirus capsid protein VP2," *Sci. Rep.* **6**, 23392 (2016).
72. N. Shadjou, M. Hasanzadeh, "Graphene and its nanostructure derivatives for use in bone tissue engineering: Recent advances," *J. Biomed. Mater. Res. Part A* **104**, 1250–1275 (2016).
73. C. Wang, C. Wu, X. Zhou, T. Han, X. Xin, J. Wu, J. Zhang, S. Guo, "Enhancing cell nucleus accumulation and DNA cleavage activity of anti-cancer drug via graphene quantum dots," *Sci. Rep.* **3**, 2852 (2013).
74. Z. Xie, C. Xing, W. Huang, T. Fan, Z. Li, J. Zhao, Y. Xiang, Z. Guo, J. Li, Z. Yang, "Ultrathin 2D nonlayered tellurium nanosheets: Facile liquid-phase exfoliation, characterization, and photoresponse with high performance and enhanced stability," *Adv. Funct. Mater.* **28**, 1705833 (2018).
75. C. Xing, Z. Xie, Z. Liang, W. Liang, T. Fan, J. S. Ponraj, S. C. Dhanabalan, D. Fan, H. Zhang, "Selenium nanosheets: 2D nonlayered selenium nanosheets: Facile synthesis, photoluminescence, and ultrafast photonics (*Advanced Optical Materials* 24/2017)," *Adv. Opt. Mater.* **5**, 1700884 (2017).
76. L. Wu, Z. Xie, L. Lu, J. Zhao, Y. Wang, X. Jiang, Y. Ge, F. Zhang, S. Lu, Z. Guo, "Few layer tin sulfide: A promising black phosphorus analogue 2D material with exceptionally large nonlinear optical response, high stability, and applications in all optical switching and wavelength conversion," *Adv. Opt. Mater.* **6**, 1700985 (2018).

77. L. Lu, Z. Liang, L. Wu, Y. X. Chen, Y. Song, S. C. Dhanabalan, J. S. Ponraj, B. Dong, Y. Xiang, F. Xing, "Few layer bismuthene: Sonochemical exfoliation, nonlinear optics and applications for ultrafast photonics with enhanced stability," *Laser Photon. Rev.* **12**, 1700221 (2018).
78. R. Balog, B. Jørgensen, L. Nilsson, M. Andersen, E. Rienks, M. Bianchi, M. Fanetti, E. Lægsgaard, A. Baraldi, S. Lizzit, "Bandgap opening in graphene induced by patterned hydrogen adsorption," *Nat. Mater.* **9**, 315 (2010).
79. C. Coletti, C. Riedl, D. S. Lee, B. Krauss, L. Patthey, K. Von Klitzing, J. H. Smet, U. Starke, "Charge neutrality and band-gap tuning of epitaxial graphene on SiC by molecular doping," *Phys. Rev. B Condens. Matter* **81**, 136–138 (2010).
80. X. Deng, Y. Wu, J. Dai, D. Kang, D. Zhang, "Electronic structure tuning and band gap opening of graphene by hole/electron codoping," *Phys. Lett. A* **375**, 3890–3894 (2011).
81. P. A. Denis, "Band gap opening of monolayer and bilayer graphene doped with aluminium, silicon, phosphorus, and sulfur," *Chem. Phys. Lett.* **492**, 251–257 (2010).
82. X. Fan, Z. Shen, A. Q. Liu, J. L. Kuo, "Band gap opening of graphene by doping small boron nitride domains," *Nanoscale* **4**, 2157–2165 (2012).
83. H. Gao, L. Wang, J. Zhao, F. Ding, J. Lu, "Band gap tuning of hydrogenated graphene: H coverage and configuration dependence," *J. Phys. Chem. C* **115**, 3236–3242 (2011).
84. C. Lin, Y. Feng, Y. Xiao, M. Dürr, X. Huang, X. Xu, R. Zhao, E. Wang, X. Z. Li, Z. Hu, "Direct observation of ordered configurations of hydrogen adatoms on graphene," *Nano Lett.* **15**, 903 (2015).
85. P. Rani, V. K. Jindal, "Designing band gap of graphene by B and N dopant atoms," *RSC Adv.* **3**, 802–812 (2012).
86. J. O. Sofo, "Graphane: A two-dimensional hydrocarbon," *Phys. Rev. B* **75**, 153401 (2007).
87. J. W. Yang, G. Lee, J. S. Kim, K. S. Kim, "Gap opening of graphene by dual FeCl3-acceptor and K-donor doping," *J. Phys. Chem. Lett.* **2**, 2577–2581 (2015).
88. I. Zanella, S. Guerini, S. B. Fagan, J. M. Filho, A. G. S. Filho, "Chemical doping-induced gap opening and spin polarization in graphene," *Phys. Rev. B* **77**, 033404 (2008).
89. A. S. George, Z. Mutlu, R. Ionescu, R. J. Wu, J. S. Jeong, H. H. Bay, Y. Chai, K. A. Mkhoyan, M. Ozkan, C. S. Ozkan, "Wafer scale synthesis and high resolution structural characterization of atomically thin MoS2 layers," *Adv. Funct. Mater.* **24**, 7461–7466 (2015).
90. K. K. Liu, W. Zhang, Y. H. Lee, Y. C. Lin, M. T. Chang, C. Y. Su, C. S. Chang, H. Li, Y. Shi, H. Zhang, "Growth of large-area and highly crystalline MoS2 thin layers on insulating substrates," *Nano Lett.* **12**, 1538–1544 (2012).
91. G. Li-Yong, Z. Qingyun, C. Yingchun, S. G. Udo, "Photovoltaic heterojunctions of fullerenes with MoS2 and WS2 monolayers," *J. Phys. Chem. Lett.* **5**, 1445–1449 (2014).
92. K. S. Novoselov, D. Jiang, F. Schedin, T. J. Booth, V. V. Khotkevich, S. V. Morozov, A. K. Geim, T. M. Rice, "Two-dimensional atomic crystals," *Proc. Natl Acad. Sci. USA* **102**, 10451–10453 (2005).
93. N. Perealópez, Z. Lin, N. R. Pradhan, A. Iñiguezrábago, A. L. Elías, A. Mccreary, J. Lou, P. M. Ajayan, H. Terrones, L. Balicas, "CVD-grown monolayered MoS2 as an effective photosensor operating at low-voltage," *2d Mater.* **1**, 011004 (2014).
94. Y. Shi, W. Zhou, A. Y. Lu, W. Fang, Y. H. Lee, A. L. Hsu, S. M. Kim, K. K. Kim, H. Y. Yang, L. J. Li, "van der Waals epitaxy of MoSâ, layers using graphene as growth templates," *Nano Lett.* **12**, 2784–2791 (2012).
95. S. Walia, S. Balendhran, H. Nili, S. Zhuiykov, G. Rosengarten, Q. H. Wang, M. Bhaskaran, S. Sriram, M. S. Strano, K. Kalantar-Zadeh, "Transition metal oxides — Thermoelectric properties," *Prog. Mater. Sci.* **58**, 1443–1489 (2013).
96. M. Ye, D. Winslow, D. Zhang, R. Pandey, Y. K. Yap, "Recent advancement on the optical properties of two-dimensional molybdenum disulfide (MoS2) thin films," *Photonics* **2**, 288–307 (2015).
97. M. Chen, H. Nam, S. Wi, G. Priessnitz, I. M. Gunawan, X. Liang, "Multibit data storage states formed in plasma-treated MoS2 transistors," *ACS Nano* **8**, 4023–4032 (2014).
98. S. Chuang, C. Battaglia, A. Azcatl, S. Mcdonnell, J. S. Kang, X. Yin, M. Tosun, R. Kapadia, H. Fang, R. M. Wallace, "MoS2 P-type transistors and diodes enabled by high workfunction MoOx contacts," *Nano Lett.* **14**, 1337 (2014).
99. J. N. Coleman, M. Lotya, A. O'Neill, S. D. Bergin, P. J. King, U. Khan, K. Young, A. Gaucher, S. De, R. J. Smith, "Two-dimensional nanosheets produced by liquid exfoliation of layered materials," *Science* **42**, 568–571 (2011).
100. J. Kang, W. Liu, K. Banerjee, "High-performance $MoS_2$ transistors with low-resistance molybdenum contacts," *Appl. Phys. Lett.* **104**, 093106-5 (2014).
101. H. Li, Q. Zhang, C. C. R. Yap, B. K. Tay, T. H. T. Edwin, A. Olivier, D. Baillargeat, "From bulk to monolayer MoS2: Evolution of Raman scattering," *Adv. Funct. Mater.* **22**, 1385–1390 (2012).

102. B. Liu, L. Chen, G. Liu, A. N. Abbas, M. Fathi, C. Zhou, "High-performance chemical sensing using Schottky-contacted chemical vapor deposition grown monolayer MoS2 transistors," *ACS Nano* **8**, 5304–5314 (2014).
103. L. Yang, K. Majumdar, H. Liu, Y. Du, H. Wu, M. Hatzistergos, P. Y. Hung, R. Tieckelmann, W. Tsai, C. Hobbs, "Chloride molecular doping technique on 2D materials: WS2 and MoS2," *Nano Lett.* **14**, 6275 (2014).
104. Z. Zeng, Z. Yin, X. Huang, H. Li, Q. He, G. Lu, F. Boey, H. Zhang, "Single layer semiconducting nanosheets: High yield preparation and device fabrication," *Angew. Chem.* **50**, 11093–11097 (2011).
105. W. Huang, C. Xing, Y. Wang, Z. Li, L. Wu, D. Ma, X. Dai, Y. Xiang, J. Li, D. Fan, "Facile fabrication and characterization of two-dimensional bismuth-(iii) sulfide nanosheets for high-performance photodetector applications under ambient conditions," *Nanoscale* **14**, 1702082 (2018).
106. X. Jiang, S. Liu, W. Liang, S. Luo, Z. He, Y. Ge, H. Wang, R. Cao, F. Zhang, Q. Wen, "Broadband nonlinear photonics in few layer MXene Ti3C2Tx (T = F, O, or OH)," *Laser Photon. Rev.* **12**, 1700229 (2017).
107. D. Ma, Y. Li, J. Yang, H. Mi, S. Luo, L. Deng, C. Yan, P. Zhang, Z. Lin, X. Ren, "Atomic layer deposition-enabled ultrastable freestanding carbon-selenium cathodes with high mass loading for sodium-selenium battery," *Nano Energy* **43**, 317–325 (2017).
108. H. Liu, K. Hu, D. Yan, R. Chen, Y. Zou, H. Liu, S. Wang, "Recent advances on black phosphorus for energy storage, catalysis, and sensor applications," *Adv. Mater.* **30**, 1800295 (2018).
109. H. Liu, A. T. Neal, Z. Zhu, Z. Luo, X. Xu, D. Tománek, P. D. Ye, "Phosphorene: An unexplored 2D semiconductor with a high hole mobility," *ACS Nano* **8**, 4033–4041 (2014).
110. A. Manjanath, A. Samanta, T. Pandey, A. K. Singh, "Semiconductor to metal transition in bilayer phosphorene under normal compressive strain," *Nanotechnology* **26**, 075701 (2015).
111. X. Peng, Q. Wei, A. Copple, "Strain-engineered direct-indirect band gap transition and its mechanism in two-dimensional phosphorene," *Phys. Rev. B* **90**, 085402 (2014).
112. J. P. Perdew, K. Burke, M. Ernzerhof, "Generalized gradient approximation made simple," *Phys. Rev. Lett.* **77**, 3865–3868 (1996).
113. E. Scalise, M. Houssa, G. Pourtois, V. Afanas'Ev, A. Stesmans, "Strain-induced semiconductor to metal transition in the two-dimensional honeycomb structure of MoS 2," *Nano Res.* **5**, 43–48 (2012).
114. C. D. Zhang, J. C. Lian, W. Yi, Y. H. Jiang, L. W. Liu, H. Hu, W. D. Xiao, S. X. Du, L. L. Sun, H. J. Gao, "Surface structures of black phosphorus investigated with scanning tunneling microscopy," *J. Phys. Chem. C* **113**, 18823–18826 (2009).
115. J. R. Choi, K. W. Yong, J. Y. Choi, A. Nilghaz, Y. Lin, J. Xu, X. Lu, "Black phosphorus and its biomedical applications," *Theranostics* **8**, 1005–1026 (2018).
116. X. Chen, G. Xu, X. Ren, Z. Li, X. Qi, K. Huang, H. Zhang, Z. Huang, J. Zhong, "A black/red phosphorus hybrid as an electrode material for high-performance Li-ion batteries and supercapacitors," *J. Mater. Chem. A* **5**, 6581–6588 (2017).
117. S. C. Dhanabalan, J. S. Ponraj, Z. Guo, S. Li, Q. Bao, H. Zhang, "Emerging trends in phosphorene fabrication towards next generation devices," *Adv. Sci.* **4**, 1600305 (2017).
118. J. Du, M. Zhang, Z. Guo, J. Chen, X. Zhu, G. Hu, P. Peng, Z. Zheng, H. Zhang, "Phosphorene quantum dot saturable absorbers for ultrafast fiber lasers," *Sci. Rep.* **7**, 42357 (2017).
119. Y. Ge, S. Chen, Y. Xu, Z. He, Z. Liang, Y. Chen, Y. Song, D. Fan, K. Zhang, H. Zhang, "Few-layer selenium-doped black phosphorus: Synthesis, nonlinear optical properties and ultrafast photonics applications," *J. Mater. Chem. C* **5**, 6129–6135 (2017).
120. Z. Guo, S. Chen, Z. Wang, Z. Yang, F. Liu, Y. Xu, J. Wang, Y. Yi, H. Zhang, L. Liao, "Metalion modified black phosphorus with enhanced stability and transistor performance," *Adv. Mater.* **29**, 1703811 (2017).
121. J. Shi, Z. Li, D. K. Sang, Y. Xiang, J. Li, S. Zhang, H. Zhang, "THz photonics in two dimensional materials and metamaterials: Properties, devices and prospects," *J. Mater. Chem. C* **6**, 1291–1306 (2018).
122. J. Sotor, G. Sobon, W. Macherzynski, P. Paletko, K. M. Abramski, "Black phosphorus saturable absorber for ultrashort pulse generation," *Appl. Phys. Lett.* **107**, 440–449 (2015).
123. X. H. Wang, J. L. Xu, S. F. Gao, Y. J. Sun, Z. J. Zhu, H. P. Xia, Z. Y. You, H. Zhang, C. Y. Tu, "Frequency stabilization of a dual-frequency Yb3+:GdAl3(BO3)4 laser via nonlinear loss modulation in black phosphorus," *Laser Phys. Lett.* **14**, 065802 (2017).
124. Y. Xu, X. F. Jiang, Y. Ge, Z. Guo, Z. Zeng, Q. H. Xu, H. Zhang, X. F. Yu, D. Fan, "Size-dependent nonlinear optical properties of black phosphorus nanosheets and their applications in ultrafast photonics," *J. Mater. Chem. C* **5**, 3007–3013 (2017).
125. J. W. Jiang, H. S. Park, "Mechanical properties of single-layer black phosphorus," *J. Phys. D Appl. Phys.* **47**, 385304 (2014).

126. Y. Poya, K. Bijandra, F. Tara, W. Canhui, A. Mohammad, T. David, I. J. Ernesto, R. F. Klie, S. K. Amin, "High-quality black phosphorus atomic layers by liquid-phase exfoliation," *Adv. Mater.* **27**, 1887–1892 (2015).
127. S. Sugai, I. Shirotani, "Raman and infrared reflection spectroscopy in black phosphorus," *Solid State Commun.* **53**, 753–755 (1985).
128. X. Wang, A. M. Jones, K. L. Seyler, V. Tran, Y. Jia, H. Zhao, H. Wang, L. Yang, X. Xu, F. Xia, "Highly anisotropic and robust excitons in monolayer black phosphorus," *Nat. Nanotechnol.* **10**, 517–521 (2015).
129. Q. Wei, X. Peng, "Superior mechanical flexibility of phosphorene and few-layer black phosphorus," *Appl. Phys. Lett.* **104**, 372–398 (2014).
130. Z. Yang, J. Hao, S. Yuan, S. Lin, H. M. Yau, J. Dai, S. P. Lau, "Field-effect transistors based on amorphous black phosphorus ultrathin films by pulsed laser deposition," *Adv. Mater.* **27**, 3748–3754 (2015).
131. Y. Xu, W. Wang, Y. Ge, H. Guo, X. Zhang, S. Chen, Y. Deng, Z. Lu, H. Zhang, "Stabilization of black phosphorous quantum dots in PMMA nanofiber film and broadband nonlinear optics and ultrafast photonics application," *Adv. Funct. Mater.* **27**, 1702437 (2017).
132. Y. Xu, J. Yuan, K. Zhang, Y. Hou, Q. Sun, Y. Yao, S. Li, Q. Bao, H. Zhang, Y. Zhang, "Field-induced *n*-doping of black phosphorus for CMOS compatible 2D logic electronics with high electron mobility," *Adv. Funct. Mater.* **27**, 1702211 (2017).
133. H. Zhang, J. Liu, Z. Chu, Z. Guo, "2 $\mu$m passively Q-switched laser based on black phosphorus," *Opt. Mater. Expr.* **6**, 2374 (2016).
134. M. C. Duch, G. R. S. Budinger, T. L. Yu, S. Soberanes, D. Urich, S. E. Chiarella, L. A. Campochiaro, A. Gonzalez, N. S. Chandel, M. C. Hersam, "Minimizing oxidation and stable nanoscale dispersion improves the biocompatibility of graphene in the lung," *Nano Lett.* **11**, 5201 (2011).
135. J. Zheng, X. Tang, Z. Yang, Z. Liang, Y. Chen, K. Wang, Y. Song, Y. Zhang, J. Ji, Y. Liu, "Few-layer phosphorene-decorated microfiber for all-optical thresholding and optical modulation," *Adv. Opt. Mater.* **5**, 1700026 (2017).
136. J. Zheng, Z. Yang, S. Chen, Z. Liang, X. Chen, R. Cao, Z. Guo, K. Wang, Y. Zhang, J. Ji, "Black phosphorus based all-optical-signal-processing: Towards high performances and enhanced stability," *ACS Photon.* **4**, 1466–1476 (2017).
137. Y. Zhou, M. Zhang, Z. Guo, L. Miao, S. T. Han, Z. Wang, X. Zhang, H. Zhang, Z. Peng, "Recent advances in black phosphorus-based photonics, electronics, sensors and energy devices," *Mater. Horizons* **4**, 997–1019 (2017).
138. W. Chen, J. Ouyang, H. Liu, M. Chen, K. Zeng, J. Sheng, Z. Liu, Y. Han, L. Wang, J. Li, L. Deng, Y. N. Liu, S. Guo, "Black phosphorus nanosheet-based drug delivery system for synergistic photodynamic/photothermal/chemotherapy of cancer," *Adv. Mater.* **29**, 1603864 (2017).
139. C. R. Dean, A. F. Young, I. Meric, C. Lee, L. Wang, S. Sorgenfrei, K. Watanabe, T. Taniguchi, P. Kim, K. L. Shepard, "Boron nitride substrates for high-quality graphene electronics," *Nat. Nanotechnol.* **5**, 722–726 (2010).
140. A. Favron, E. Gaufrès, F. Fossard, A. L. Phaneufl'Heureux, N. Y. Tang, P. L. Lévesque, A. Loiseau, R. Leonelli, S. Francoeur, R. Martel, "Photooxidation and quantum confinement effects in exfoliated black phosphorus," *Nat. Mater.* **14**, 826–832 (2015).
141. G. H. Lee, Y. J. Yu, C. Lee, C. Dean, K. L. Shepard, P. Kim, J. Hone, "Electron tunneling through atomically flat and ultrathin hexagonal boron nitride," *Appl. Phys. Lett.* **99**, 666 (2011).
142. Y. Wang, J. Z. Ou, S. Balendhran, A. F. Chrimes, M. Mortazavi, D. D. Yao, M. R. Field, K. Latham, V. Bansal, J. R. Friend, "Electrochemical control of photoluminescence in two-dimensional MoS(2) nanoflakes," *ACS Nano* **7**, 10083–10093 (2013).
143. J. D. Wood, S. A. Wells, D. Jariwala, K. S. Chen, E. Cho, V. K. Sangwan, X. Liu, L. J. Lauhon, T. J. Marks, M. C. Hersam, "Effective passivation of exfoliated black phosphorus transistors against ambient degradation," *Nano Lett.* **14**, 6964–6970 (2014).
144. Z. Zeng, T. Sun, J. Zhu, X. Huang, Z. Yin, G. Lu, Z. Fan, Q. Yan, H. H. Hng, H. Zhang, "An effective method for the fabrication of few-layer-thick inorganic nanosheets," *Angew. Chem.* **124**, 9186–9190 (2012).
145. N. M. Latiff, W. Z. Teo, Z. Sofer, A. C. Fisher, M. Pumera, "The cytotoxicity of layered black phosphorus," *Chemistry* **21**, 13991–13995 (2015)
146. Kenry, C. T. Lim, "Biocompatibility and nanotoxicity of layered two-dimensional nanomaterials," *ChemNanoMat* **3**, 5–16 (2017).
147. J. Shao, H. Xie, H. Huang, Z. Li, Z. Sun, Y. Xu, Q. Xiao, X. F. Yu, Y. Zhao, H. Zhang, H. Wang, P. K. Chu, "Biodegradable black phosphorus-based nanospheres for *in vivo* photothermal cancer therapy," *Nat. Commun.* **7**, 12967 (2016).
148. X. Zhang, Z. Zhang, S. Zhang, D. Li, W. Ma, C. Ma, F. Wu, Q. Zhao, Q. Yan, B. Xing, "Size effect on the cytotoxicity of layered black phosphorus and underlying mechanisms," *Small* **13**, 1701210 (2017).

149. X. Mu, J. Y. Wang, X. Bai, F. Xu, H. Liu, J. Yang, Y. Jing, L. Liu, X. Xue, H. Dai, Q. Liu, Y. M. Sun, C. Liu, X. D. Zhang, "Black phosphorus quantum dot induced oxidative stress and toxicity in living cells and mice," *ACS Appl. Mater. Interf.* **9**, 20399–20409 (2017).
150. S.-J. Song, Y. Shin, H. Lee, B. Kim, D.-W. Han, D. Lim, "Dose- and time-dependent cytotoxicity of layered black phosphorus in fibroblastic cells," *Nanomaterials* **8**, 408 (2018).
151. J. Homola, "Surface plasmon resonance sensors for detection of chemical and biological species," *Chem. Rev.* **39**, 462–493 (2008).
152. H. Im, H. Shao, I. P. Yong, V. M. Peterson, C. M. Castro, R. Weissleder, H. Lee, "Label-free detection and molecular profiling of exosomes with a nano-plasmonic sensor," *Nat. Biotechnol.* **32**, 490–495 (2014).
153. R. Jha, A. K. Sharma, "Chalcogenide glass prism based SPR sensor with Ag-Au bimetallic nanoparticle alloy in infrared wavelength region," *J. Opt. A Pure Appl. Opt.* **11**, 045502 (2009).
154. A. Lahav, M. Auslender, I. Abdulhalim, "Sensitivity enhancement of guided-wave surface-plasmon resonance sensors," *Opt. Lett.* **33**, 2539–2541 (2008).
155. C. F. Mandenius, R. Wang, A. Aldén, M. G. Bergström, S. Thébault, C. Lutsch, S. Ohlson, "Monitoring of influenza virus hemagglutinin in process samples using weak affinity ligands and surface plasmon resonance," *Anal. Chim. Acta* **623**, 66–75 (2008).
156. E. Mauriz, A. Calle, J. J. Manclús, A. Montoya, L. M. Lechuga, "Multi-analyte SPR immunoassays for environmental biosensing of pesticides," *Anal. Bioanal. Chem.* **387**, 1449–1458 (2007).
157. M. Piliarik, L. Párová, J. Homola, "High-throughput SPR sensor for food safety," *Biosens. Bioelectron.* **24**, 1399–1404 (2009).
158. V. Shpacovitch, V. Temchura, M. Matrosovich, J. Hamacher, J. Skolnik, P. Libuschewski, D. Siedhoff, F. Weichert, P. Marwedel, H. Müller, "Application of surface plasmon resonance imaging technique for the detection of single spherical biological submicrometer particles," *Anal. Biochem.* **486**, 62–69 (2015).
159. A. Turner, "Biosensors: Then and now," *Trends Biotechnol.* **31**, 119–120 (2013).
160. A. W. Wark, H. J. Lee, R. M. Corn, "Long-range surface plasmon resonance imaging for bioaffinity sensors," *Anal. Chem.* **77**, 3904–3907 (2005).
161. Y. Chen, R. Ren, H. Pu, J, Chang, S. Mao, J. Chen, "Field-effect transistor biosensors with two-dimensional black phosphorus nanosheets," *Biosens. Bioelectron.* **89**, 505–510 (2017).
162. C. C. Mayorga-Martinez, N. Mohamad Latiff, A. Y. Eng, Z. Sofer, M. Pumera, "Black phosphorus nanoparticle labels for immunoassays via hydrogen evolution reaction mediation," *Anal. Chem.* **88**, 10074–10079 (2016).
163. V. Kumar, J. R. Brent, M. Shorie, H. Kaur, G. Chadha, A. G. Thomas, E. A. Lewis, A. P. Rooney, L. Nguyen, X. L. Zhong, M. G. Burke, S. J. Haigh, A. Walton, P. D. McNaughter, A. A. Tedstone, N. Savjani, C. A. Muryn, P. O'Brien, A. K. Ganguli, D. J. Lewis, P. Sabherwal, "Nanostructured aptamer-functionalized black phosphorus sensing platform for label-free detection of myoglobin, a cardiovascular disease biomarker," *ACS Appl. Mater. Interf.* **8**, 22860–22868 (2016).
164. W. Gu, Y. Yan, X. Pei, C. Zhang, C. Ding, Y. Xian, "Fluorescent black phosphorus quantum dots as label-free sensing probes for evaluation of acetylcholinesterase activity," *Sens. Actuat. B: Chem.* **250**, 601–607 (2017).
165. M. Lee, Y. H. Park, E. B. Kang, A. Chae, Y. Choi, S. Jo, Y. J. Kim, S.-J. Park, B. Min, T. K. An, J. Lee, S.-I. In, S. Y. Kim, S. Y. Park, I. In, "Highly efficient visible blue-emitting black phosphorus quantum dot: Mussel-inspired surface functionalization for bioapplications," *ACS Omega* **2**, 7096–7105 (2017).
166. Y. T. Yew, Z. Sofer, C. C. Mayorga-Martinez, M. Pumera, "Black phosphorus nanoparticles as a novel fluorescent sensing platform for nucleic acid detection," *Mater. Chem. Front.* **1**, 1130–1136 (2017).
167. T. D. Craggs, "Green fluorescent protein: Structure, folding and chromophore maturation," *Chem. Soc. Rev.* **38**, 2865–2875 (2009).
168. J. R. Enterina, L. Wu, R. E. Campbell, "Emerging fluorescent protein technologies," *Curr. Opin. Chem. Biol.* **27**, 10–17 (2015).
169. Y. Hong, J. W. Lam, B. Z. Tang, "Aggregation-induced emission: Phenomenon, mechanism and applications," *ChemInform* **40**, 4332–4353 (2009).
170. J. Mei, N. L. Leung, R. T. Kwok, J. W. Lam, B. Z. Tang, "Aggregation-induced emission: Together we shine, united we soar!," *Chem. Rev.* **115**, 11718–11940 (2015).
171. J. Qian, D. Wang, F. Cai, Q. Zhan, Y. Wang, S. He, "Photosensitizer encapsulated organically modified silica nanoparticles for direct two-photon photodynamic therapy and *in vivo* functional imaging," *Biomaterials* **33**, 4851–4860 (2012).
172. T. Sun, Y. S. Zhang, B. Pang, D. C. Hyun, M. Yang, Y. Xia, "Engineered nanoparticles for drug delivery in cancer therapy," *Angew. Chem.* **53**, 12320–12364 (2015).
173. D. Wang, J. Qian, S. He, J. S. Park, K. S. Lee, S. Han, Y. Mu, "Aggregation-enhanced fluorescence

in PEGylated phospholipid nanomicelles for *in vivo* imaging," *Biomaterials* **32**, 5880–5888 (2011).
174. D. Wang, J. Qian, W. Qin, A. Qin, B. Z. Tang, S. He, "Biocompatible and photostable AIE dots with red emission for *in vivo* two-photon bioimaging," *Sci. Rep.* **4**, 4279 (2014).
175. X. D. Wang, O. S. Wolfbeis, R. J. Meier, "Luminescent probes and sensors for temperature," *Chem. Soc. Rev.* **42**, 7834–7869 (2013).
176. Y. Zhang, J. Qian, D. Wang, Y. Wang, S. He, "Multifunctional gold nanorods with ultrahigh stability and tunability for *in vivo* fluorescence imaging, SERS detection, and photodynamic therapy," *Angew. Chem.* **125**, 1186–1189 (2013).
177. Z. Zhao, B. He, B. Z. Tang, "Aggregation-induced emission of siloles," *Chem. Sci.* **6**, 5347–5365 (2015).
178. P. P. Adiseshaiah, R. M. Crist, S. S. Hook, S. E. McNeil, "Nanomedicine strategies to overcome the pathophysiological barriers of pancreatic cancer," *Nat. Rev. Clin. Oncol.* **13**, 750–765 (2016).
179. V. P. Chauhan, R. K. Jain, "Strategies for advancing cancer nanomedicine," *Nat. Mater.* **12**, 958–962 (2013).
180. X. B. Cheng, K. Shiro, K. Atsuhiro, H. Keiji, S. Norihiro, "Hyaluronan stimulates pancreatic cancer cell motility," *Oncotarget* **7**, 4829–4840 (2016).
181. P. Couvreur, "Nanoparticles in drug delivery: Past, present and future," *Adv. Drug Deliv. Rev.* **65**, 21–23 (2013).
182. B. Diop-Frimpong, V. P. Chauhan, S. Krane, Y. Boucher, R. K. Jain, "Losartan inhibits collagen I synthesis and improves the distribution and efficacy of nanotherapeutics in tumors," *Proc. National Acad. Sci. USA* **108**, 2909–2914 (2011).
183. R. Guo, J. Gu, Z. Zhang, Y. Wang, C. Gu, "MicroRNA-410 functions as a tumor suppressor by targeting angiotensin II type 1 receptor in pancreatic cancer," *IUBMB Life* **67**, 42–53 (2015).
184. R. M. Hoffman, M. Bouvet, "Nanoparticle albumin-bound-paclitaxel: A limited improvement under the current therapeutic paradigm of pancreatic cancer," *Exp. Opin. Pharmacother.* **16**, 943–947 (2015).
185. S. Lunardi, R. J. Muschel, T. B. Brunner, "The stromal compartments in pancreatic cancer: Are there any therapeutic targets?," *Cancer Lett.* **343**, 147–155 (2014).
186. E. R. Manuel, J. Chen, M. D'Apuzzo, M. G. Lampa, T. I. Kaltcheva, C. B. Thompson, T. Ludwig, V. Chung, D. J. Diamond, "Salmonella-based therapy targeting indoleamine 2,3-dioxygenase coupled with enzymatic depletion of tumor hyaluronan induces complete regression of aggressive pancreatic tumors," *Cancer Immunol. Res.* **3**, 1096 (2015).
187. C. J. Whatcott, H. Hanl, D. D. V. Hoff, "Orchestrating the tumor microenvironment to improve survival for patients with pancreatic cancer normalization, not destruction," *Cancer J.* **21**, 299–306 (2015).
188. G. Yin, J. Haendeler, C. Yan, B. C. Berk, "GIT1 functions as a scaffold for MEK1-extracellular signal-regulated kinase 1 and 2 activation by angiotensin II and epidermal growth factor," *Mol. Cell. Biol.* **24**, 875–885 (2004).
189. J. Shao, C. Ruan, H. Xie, Z. Li, H. Wang, P. K. Chu, X.-F. Yu, "Black-phosphorus-incorporated hydrogel as a sprayable and biodegradable photothermal platform for postsurgical treatment of cancer," *Adv. Sci.* **5**, 1700848 (2018).
190. M. Qiu, D. Wang, W. Liang, L. Liu, Y. Zhang, X. Chen, D. K. Sang, C. Xing, Z. Li, B. Dong, F. Xing, D. Fan, S. Bao, H. Zhang, Y. Cao, "Novel concept of the smart NIR-light-controlled drug release of black phosphorus nanostructure for cancer therapy," *Proc. Natl Acad. Sci. USA* **115**, 501–506 (2018).
191. C. Sun, L. Wen, J. Zeng, Y. Wang, Q. Sun, L. Deng, C. Zhao, Z. Li, "One-pot solventless preparation of PEGylated black phosphorus nanoparticles for photoacoustic imaging and photothermal therapy of cancer," *Biomaterials* **91**, 81–89 (2016).
192. Z. Sun, Y. Zhao, Z. Li, H. Cui, Y. Zhou, W. Li, W. Tao, H. Zhang, H. Wang, P. K. Chu, X. F. Yu, "TiL4 -coordinated black phosphorus quantum dots as an efficient contrast agent for *in vivo* photoacoustic imaging of cancer," *Small* **13**, 1602896 (2017).
193. G. Yang, Z. Liu, Y. Li, Y. Hou, X. Fei, C. Su, S. Wang, Z. Zhuang, Z. Guo, "Facile synthesis of black phosphorus-Au nanocomposites for enhanced photothermal cancer therapy and surface-enhanced Raman scattering analysis," *Biomater. Sci.* **5**, 2048–2055 (2017).
194. G. Huang, X. Zhu, H. Li, L. Wang, X. Chi, J. Chen, X. Wang, Z. Chen, J. Gao, "Facile integration of multiple magnetite nanoparticles for theranostics combining efficient MRI and thermal therapy," *Nanoscale* **7**, 2667–2675 (2015).
195. M. Zhou, R. Zhang, M. Huang, W. Lu, S. Song, M. P. Melancon, M. Tian, D. Liang, C. Li, "A chelator-free multifunctional [64Cu]CuS nanoparticle platform for simultaneous micro-PET/CT imaging and photothermal ablation therapy," *J. Am. Chem. Soc.* **132**, 15351–15358 (2010).

196. H. Abrahamse, M. R. Hamblin, "New photosensitizers for photodynamic therapy," *Biochem. J.* **473**, 347 (2016).
197. B. N. And, M. A. Elsayed, "Preparation and growth mechanism of gold nanorods (NRs) using seed-mediated growth method," *Chem. Mater.* **15**, 1957–1962 (2003).
198. A. A. Bhirde, V. Patel, J. Gavard, G. Zhang, A. A. Sousa, A. Masedunskas, R. D. Leapman, R. Weigert, J. S. Gutkind, J. F. Rusling, "Targeted killing of cancer cells in vivo and in vitro with EGF-directed carbon nanotube-based drug delivery," *ACS Nano* **3**, 307 (2009).
199. F. Bryden, A. Maruani, J. Rodrigues, M. Cheng, H. Savoie, A. Beeby, V. Chudasama, R. W. Boyle, "Assembly of high-potency photosensitizer-antibody conjugates through application of dendron multiplier technology," *Bioconj. Chem.* **29**, 176 (2018).
200. S. S. Chou, B. Kaehr, J. Kim, B. M. Foley, M. De, P. E. Hopkins, J. Huang, C. J. Brinker, V. P. Dravid, "Chemically exfoliated MoS2 as near-infrared photothermal agents," *Angew. Chem.* **125**, 4254–4258 (2013).
201. T. A. Debele, S. L. Mekuria, H. C. Tsai, "A pH-sensitive micelle composed of heparin, phospholipids, and histidine as the carrier of photosensitizers: Application to enhance photodynamic therapy of cancer," *Int. J. Biol. Macromol.* **98**, 125 (2017).
202. P. Drake, H. J. Cho, P. S. Shih, C. H. Kao, K. F. Lee, C. H. Kuo, X. Z. Lin, Y. J. Lin, "Gd-doped iron-oxide nanoparticles for tumour therapy via magnetic field hyperthermia," *J. Mater. Chem.* **17**, 4914–4918 (2007).
203. N. R. Gemmell, A. Mccarthy, M. M. Kim, I. Veilleux, T. C. Zhu, G. S. Buller, B. C. Wilson, R. H. Hadfield, "A compact fiber-optic probe-based singlet oxygen luminescence detection system," *J. Biophoton.* **10**, 320 (2017).
204. X. Huang, S. Tang, X. Mu, Y. Dai, G. Chen, Z. Zhou, F. Ruan, Z. Yang, N. Zheng, "Freestanding palladium nanosheets with plasmonic and catalytic properties," *Nat. Nanotechnol.* **6**, 28–32 (2011).
205. D. Jaque, L. M. Martínez, B. R. Del, P. Harogonzalez, A. Benayas, J. L. Plaza, E. R. Martín, J. S. García, "Nanoparticles for photothermal therapies," *Nanoscale* **6**, 9494–9530 (2014).
206. H. Koo, H. Lee, S. Lee, K. H. Min, M. S. Kim, D. S. Lee, Y. Choi, I. C. Kwon, K. Kim, S. Y. Jeong, " *In vivo* tumor diagnosis and photodynamic therapy via tumoral pH-responsive polymeric micelles," *Chem. Commun.* **46**, 5668–5670 (2010).
207. F. G. Le, V. Sol, C. Ouk, P. Arnoux, C. Frochot, T. S. Ouk, "Enhanced photobactericidal and targeting properties of a cationic porphyrin following attachment of B. Polymyxin," *Bioconj. Chem.* **28**, 2493–2506 (2018).
208. D. Li, L. Li, P. Li, Y. Li, X. Chen, "Apoptosis of HeLa cells induced by a new targeting photosensitizer-based PDT via a mitochondrial pathway and ER stress," *Oncotargets Therapy* **8**, 703–711 (2015).
209. J. Li, F. Jiang, B. Yang, X. R. Song, Y. Liu, H. H. Yang, D. R. Cao, W. R. Shi, G. N. Chen, "Topological insulator bismuth selenide as a theranostic platform for simultaneous cancer imaging and therapy," *Sci. Rep.* **3**, 1998 (2013).
210. Z. Liu, K. Rakhra, S. Sherlock, A. Goodwin, X. Chen, Q. Yang, D. W. Felsher, H. Dai, "Supramolecular stacking of doxorubicin on carbon nanotubes for *in vivo* cancer therapy," *Angew. Chem.* **121**, 7804–7808 (2010).
211. K. K. Lo, C. K. Chung, N. Zhu, "Synthesis, photophysical and electrochemical properties, and biological labeling studies of cyclometalated iridium-(III) bis(pyridylbenzaldehyde) complexes: Novel luminescent cross-linkers for biomolecules," *Chemistry* **9**, 475–483 (2010).
212. A. Nakagawa, Y. Hisamatsu, S. Moromizato, M. Kohno, S. Aoki, "Synthesis and photochemical properties of pH responsive tris-cyclometalated iridium(III) complexes that contain a pyridine ring on the 2-phenylpyridine ligand," *Inorg. Chem.* **53**, 409–422 (2014).
213. C. A. Poland, R. Duffin, I. Kinloch, A. Maynard, W. A. Wallace, A. Seaton, V. Stone, S. Brown, W. Macnee, K. Donaldson, "Carbon nanotubes introduced into the abdominal cavity of mice show asbestos-like pathogenicity in a pilot study," *Nat. Nanotechnol.* **3**, 423–428 (2008).
214. N. K. Prasad, K. Rathinasamy, D. Panda, D. Bahadur, "Mechanism of cell death induced by magnetic hyperthermia with nanoparticles of γ-MnxFe2–xO3 synthesized by a single step process," *J. Mater. Chem.* **17**, 5042–5051 (2007).
215. G. Rahmathulla, P. F. Recinos, K. Kamian, A. M. Mohammadi, M. S. Ahluwalia, G. H. Barnett, "MRI-guided laser interstitial thermal therapy in neuro-oncology: A review of its current clinical applications," *Oncology* **87**, 67–82 (2014).
216. V. Rapozzi, D. Ragno, A. Guerrini, C. Ferroni, P. E. Della, D. Cesselli, G. Castoria, D. M. Di, E. Saracino, V. Benfenati, "Androgen receptor targeted conjugate for bimodal photodynamic therapy of prostate cancer *in vitro*," *Bioconj. Chem.* **26**, 1662 (2015).
217. K. Yang, L. Feng, X. Shi, Z. Liu, "Nano-graphene in biomedicine: Theranostic applications," *Chem. Soc. Rev.* **42**, 530–547 (2012).
218. Z. Yu, Q. Sun, W. Pan, N. Li, B. Tang, "A near-infrared triggered nanophotosensitizer inducing

Domino effect on mitochondrial reactive oxygen species burst for cancer therapy," *ACS Nano* **9**, 11064–11074 (2015).

219. A. Yuan, J. Wu, X. Tang, L. Zhao, F. Xu, Y. Hu, "Application of near-infrared dyes for tumor imaging, photothermal, and photodynamic therapies," *J. Pharmaceut. Sci.* **102**, 6–28 (2012).
220. Z. Hu, Y. Sim, O. L. Kon, W. H. Ng, A. J. Ribeiro, M. J. Ramos, P. A. Fernandes, R. Ganguly, B. Xing, F. García, E. K. Yeow, "Unique triphenylphosphonium derivatives for enhanced mitochondrial uptake and photodynamic therapy," *Bioconj. Chem.* **28**, 590 (2017).
221. P. Zhang, C. Hu, W. Ran, J. Meng, Q. Yin, Y. Li, "Recent progress in light-triggered nanotheranostics for cancer treatment," *Theranostics* **6**, 948–968 (2016).
222. H. Zhao, D. Xing, Q. Chen, "New insights of mitochondria reactive oxygen species generation and cell apoptosis induced by low dose photodynamic therapy," *Eur. J. Cancer* **47**, 2750–2761 (2011).
223. Z. Sun, H. Xie, S. Tang, X. F. Yu, Z. Guo, J. Shao, H. Zhang, H. Huang, H. Wang, P. K. Chu, "Ultrasmall black phosphorus quantum dots: Synthesis and use as photothermal agents," *Angewandte Chemie* **54**, 11526–11530 (2015).
224. H. Fu, Z. Li, H. Xie, Z. Sun, B. Wang, H. Huang, G. Han, H. Wang, P. K. Chu, X.-F. Yu, "Different-sized black phosphorus nanosheets with good cytocompatibility and high photothermal performance," *RSC Adv.* **7**, 14618–14624 (2017).
225. C. Xing, S. Chen, M. Qiu, X. Liang, Q. Liu, Q. Zou, Z. Li, Z. Xie, D. Wang, B. Dong, L. Liu, D. Fan, H. Zhang, "Conceptually novel black phosphorus/cellulose hydrogels as promising photothermal agents for effective cancer therapy," *Adv. Healthcare Mater.* **7**, 1701510 (2018).
226. C. Xing, G. Jing, X. Liang, M. Qiu, Z. Li, R. Cao, X. Li, D. Fan, H. Zhang, "Graphene oxide/black phosphorus nanoflake aerogels with robust thermostability and significantly enhanced photothermal properties in air," *Nanoscale* **9**, 8096–8101 (2017).
227. Y. Zhao, L. Tong, Z. Li, N. Yang, H. Fu, L. Wu, H. Cui, W. Zhou, J. Wang, H. Wang, P. K. Chu, X.-F. Yu, "Stable and multifunctional dye-modified black phosphorus nanosheets for near-infrared imaging-guided photothermal therapy," *Chem. Mater.* **29**, 7131–7139 (2017).
228. B. Yang, J. Yin, Y. Chen, S. Pan, H. Yao, Y. Gao, J. Shi, "2D-black-phosphorus-reinforced 3D-printed scaffolds: A stepwise countermeasure for osteosarcoma," *Adv. Mater.* **30**, 1705611 (2018).
229. W. Chen, J. Ouyang, X. Yi, Y. Xu, C. Niu, W. Zhang, L. Wang, J. Sheng, L. Deng, Y. N. Liu, S. Guo, "Black phosphorus nanosheets as a neuroprotective nanomedicine for neurodegenerative disorder therapy," *Adv. Mater.* **30**, 1703458 (2018).
230. H. Wang, X. Yang, W. Shao, S. Chen, J. Xie, X. Zhang, J. Wang, Y. Xie, "Ultrathin black phosphorus nanosheets for efficient singlet oxygen generation," *J. Am. Chem. Soc.* **137**, 11376–11382 (2015).
231. T. Guo, Y. Wu, Y. Lin, X. Xu, H. Lian, G. Huang, J. Z. Liu, X. Wu, H. H. Yang, "Black phosphorus quantum dots with renal clearance property for efficient photodynamic therapy," *Small* **14**, 1702815 (2018).
232. L. Chen, C. Zhang, L. Li, H. Wu, X. Wang, S. Yan, Y. Shi, M. Xiao, "Ultrafast carrier dynamics and efficient triplet generation in black phosphorus quantum dots," *J. Phys. Chem. C* **121**, 12972–12978 (2017).
233. L. Tan, J. Li, X. Liu, Z. Cui, X. Yang, K. W. K. Yeung, H. Pan, Y. Zheng, X. Wang, S. Wu, "In situ disinfection through photoinspired radical oxygen species storage and thermal-triggered release from black phosphorous with strengthened chemical stability," *Small* **14**, 1703197 (2018).
234. X. Tang, Y. Liang, Y. Zhu, C. Xie, A. Yao, L. Chen, Q. Jiang, T. Liu, X. Wang, Y. Qian, "Anti-transferrin receptor-modified amphotericin B-loaded PLA-PEG nanoparticles cure *Candidal meningitis* and reduce drug toxicity," *Int. J. Nanomed.* **10**, 6227–6241 (2015).
235. S. Tortorella, T. C. Karagiannis, "Transferrin receptor-mediated endocytosis: A useful target for cancer therapy," *J. Membr. Biol.* **247**, 291–307 (2014).
236. S. Gao, J. Li, C. Jiang, B. Hong, B. Hao, "Plasmid pORF-hTRAIL targeting to glioma using transferrin-modified polyamidoamine dendrimer," *Drug Des. Develop. Therapy* **10**, 1–11 (2016).
237. J. A. Loureiro, B. Gomes, M. A. Coelho, C. P. M. Do, S. Rocha, "Targeting nanoparticles across the blood–brain barrier with monoclonal antibodies," *Nanomedicine* **9**, 709–722 (2014).
238. M. Porru, S. Zappavigna, G. Salzano, A. Luce, A. Stoppacciaro, M. L. Balestrieri, S. Artuso, S. Lusa, G. D. Rosa, C. Leonetti, "Medical treatment of orthotopic glioblastoma with transferrin-conjugated nanoparticles encapsulating zoledronic acid," *Oncotarget* **5**, 10446–10459 (2014).
239. T. R. Daniels, T. Delgado, G. Helguera, M. L. Penichet, "The transferrin receptor part II: Targeted delivery of therapeutic agents into cancer cells," *Clin. Immunol.* **121**, 159–176 (2006).
240. W. Tao, X. Zhu, X. Yu, X. Zeng, Q. Xiao, X. Zhang, X. Ji, X. Wang, J. Shi, H. Zhang, L. Mei, "Black phosphorus nanosheets as a robust delivery platform for cancer theranostics," *Adv. Mater.* **29**, 1603276 (2017).

241. S. Wang, J. Weng, X. Fu, J. Lin, W. Fan, N. Lu, J. Qu, S. Chen, T. Wang, P. Huang, "Black phosphorus nanosheets for mild hyperthermia-enhanced chemotherapy and chemo-photothermal combination therapy," *Nanotheranostics* **1**, 208–216 (2017).

242. F. Yin, K. Hu, S. Chen, D. Wang, J. Zhang, M. Xie, D. Yang, M. Qiu, H. Zhang, Z.-G. Li, "Black phosphorus quantum dot based novel siRNA delivery systems in human pluripotent teratoma PA-1 cells," *J. Mater. Chem. B* **5**, 5433–5440 (2017).